

Can Milankovitch Orbital Variations Initiate the Growth of Ice Sheets in a General Circulation Model?

D. RIND AND D. PETEET

Goddard Space Flight Center, Institute for Space Studies, New York

G. KUKLA

*Lamont-Doherty Geological Observatory of Columbia University,
Palisades, New York*

The Goddard Institute for Space Studies climate model is used to investigate whether the growth of ice sheets could have been initiated by solar insolation variations. Three different orbital configurations are used, corresponding to 116 and 106 kyr B.P., and a modified insolation field with greater reductions in summer insolation at high northern latitudes. The time periods chosen are those in which geophysical evidence suggests ice sheets may have been growing rapidly. The reduced summer insolation field characteristic of all the experiments is thought to be a necessary condition for allowing snow to last through the summer, and ice sheets to build. The results show that the model fails to maintain snow cover through the summer at locations of suspected initiation of the major ice sheets, despite the reduced summer and fall insolation. When 10-m-thick ice was inserted in all locations where continental ice sheets existed during the Last Glacial Maximum, the model failed to maintain it as well, producing energy and mass imbalances which would remove the ice within 5 years. Only when the ocean surface temperatures were adjusted to their peak ice age values was the model able to keep any of the additional ice, and then only in a very restricted region of northern Baffin Island. The experiments indicate there is a wide discrepancy between the model's response to Milankovitch perturbations and the geophysical evidence of ice sheet initiation. As the model failed to grow or sustain low-altitude ice during the time of high-latitude maximum solar radiation reduction (120–110 kyr B.P.), it is unlikely it could have done so at any other time within the last several hundred thousand years. If the model results are correct, it indicates that the growth of ice occurred in an extremely ablativ environment, and thus demanded some complicated strategy, or else some other climate forcing occurred in addition to the orbital variation influence (and CO₂ reduction), which would imply we do not really understand the cause of the ice ages and the Milankovitch connection. If the model is not nearly sensitive enough to climate forcing, it could have implications for projections of future climate change.

1. INTRODUCTION

The observations of *Mesolella et al.* [1969] and *Hays et al.* [1976] showed that the climatic record from raised coral reefs and deep-sea sediments varied with periodicities which matched those of the Earth's orbital variations. *Kukla et al.* [1981] described how the orbital configurations seemed to match up with gross climate variations for the last 150 millennia or so. As a result of these and other geological studies, the consensus exists that orbital variations are responsible for initiating glacial and interglacial climatic regimes. The most obvious difference between these two regimes, the existence of subpolar continental ice sheets, appears related to solar insolation at northern hemisphere high latitudes in summer. For example, solar insolation at these latitudes in August and September was reduced, compared with today's values, around 116,000 years before the present (116 kyr B.P.), during the time when ice growth apparently began, and it was increased around 10 kyr B.P. during a time of rapid ice sheet retreat [e.g., *Berger*, 1978] (Figure 1). There are still considerable uncertainties over some aspects of the correlation of the climate record with orbital variations, such as the unexplained large variance in the 100-kyr frequency band and the reason behind the

initiation of ice buildup around 2 m.y. ago. Nevertheless, the basic relationship between orbital perturbations and climate has gained general acceptance.

Are the solar radiation variations themselves sufficient to produce or destroy the continental ice sheets? The July solar radiation incident at 50° and 60°N over the past 170 kyr is shown in Figure 1, along with August and September values at 50°N (as shown by the example for July, values at the various latitudes of concern for ice age initiation all have similar insolation fluctuations). The peak variations are of the order of 10%, which if translated with an equal percentage into surface air temperature changes would be of the order of 30°C. This would certainly be sufficient to allow snow to remain throughout the summer in extreme northern portions of North America, where July surface temperatures today are only about 10°C above freezing. However, the direct translation ignores all of the other features which influence surface air temperature during summer, such as cloud cover and albedo variations, long wave radiation, surface flux effects, and advection.

The climatic change which would be necessary is most uncertain for the ice sheets which likely developed at low elevation, in particular, the Laurentide ice sheet, requiring descent of the freezing line all the way to the surface. The uncertainty is amplified because disagreement exists on the location of the Laurentide ice sheet inception [cf. *Ives et al.*, 1975; *Williams*, 1979; *Andrews*, 1987]. Various possibilities

Copyright 1989 by the American Geophysical Union.

Paper number 89JD00885.
0148-0227/89/89JD-00885\$05.00

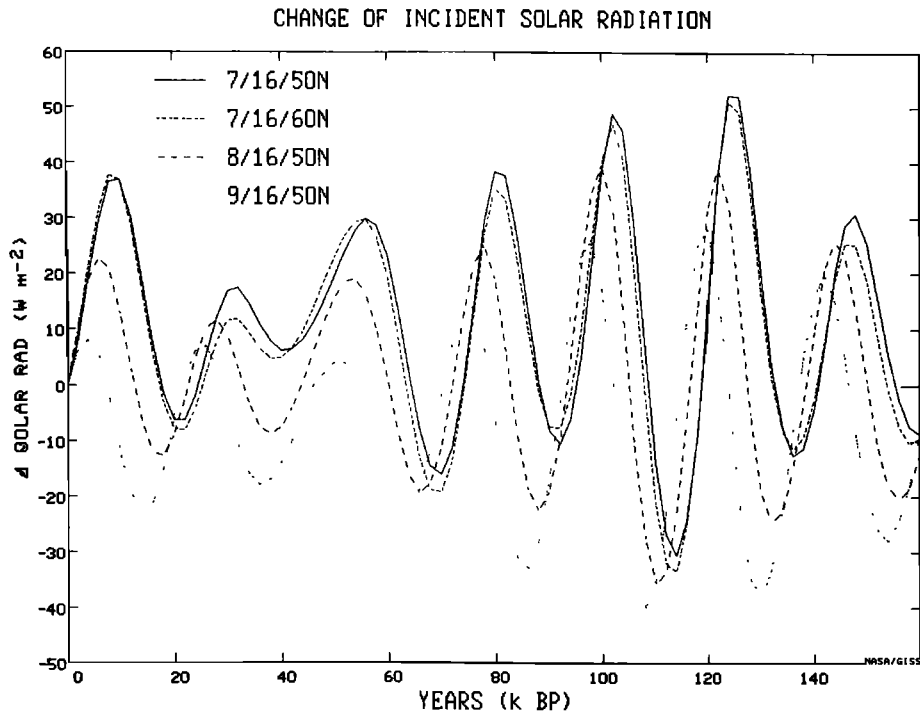


Fig. 1. Change in the incident solar radiation during the past 160,000 years in July, August, and September at 50°N, and for July at 60°N.

have been suggested, including Baffin Island in the northeast portion of Canada (Figure 2), further south in the Labrador-Ungava plateau, in the Keewatin area just northwest of Hudson Bay, and even the cold continental region further west. The possible importance of sea ice has also been raised [e.g., Denton and Hughes, 1981]. Estimates of the necessary

cooling are thus site specific and are also model specific; values range from -5° to $-12^{\circ}C$ (see the discussion by Williams [1979]).

Various energy balance climate models have been used to assess how much cooling would be associated with changed orbital parameters. As the initiation of ice growth will alter

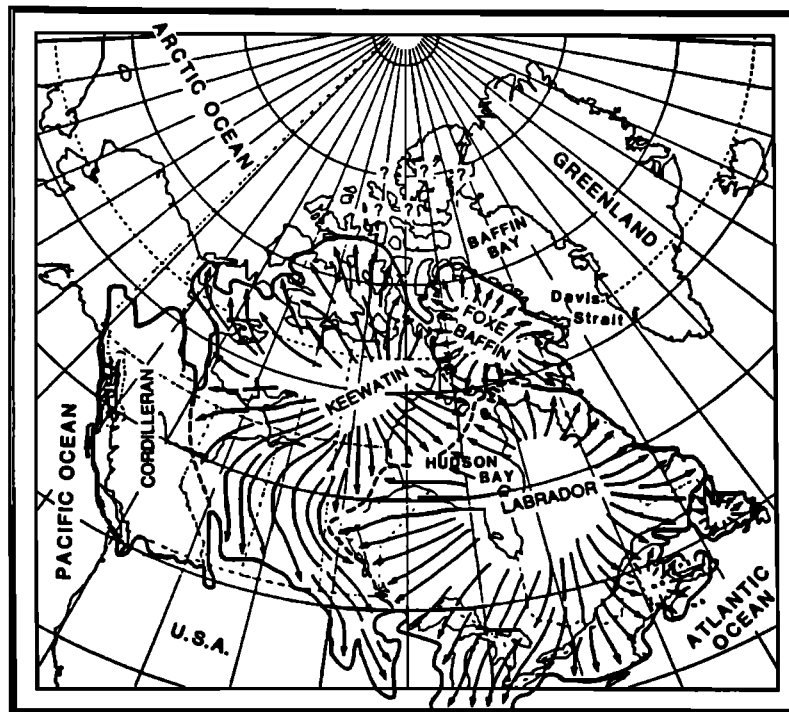


Fig. 2. North American glacial ice sheets and potential source locations [from Prest, 1984].

the surface albedo and provide feedback to the climate change, the models also have to include crude estimates of how ice cover will change with climate. With the proper tuning of parameters, some of which is justified on observational grounds, the models can be made to simulate the gross glacial/interglacial climate changes [e.g., *Schneider and Thompson, 1979; Suarez and Held, 1979; Oerlemans, 1980; Birchfield and Weertman, 1982; Pollard, 1983*]. However, these models do not calculate from first principles all the various influences on surface air temperature noted above, nor do they contain a hydrologic cycle which would allow snow cover to be generated or increase. The actual processes associated with allowing snow cover to remain through the summer will involve complex hydrologic and thermal influences, for which simple models can only provide gross approximations.

The major drawback with using more complicated models, such as general circulation models (GCMs) is that ice growth presumably occurs slowly over time, and it is computationally impractical to simulate conditions over thousands of years. Furthermore, GCMs do not contain the sophisticated ice dynamics models to properly develop or destroy ice sheets. Nevertheless, given the uncertainties which surround the growth of low-altitude ice sheets, such as the ice cap in Labrador-Ungava [e.g., *Barry et al., 1975*], it is interesting to examine what a GCM depicts for the snow/ice sheet mass and energy balances as orbital parameters are changed.

We have thus used the Goddard Institute for Space Studies (GISS) GCM for a series of experiments in which orbital parameters, atmospheric composition, and sea surface temperatures are changed. We examine how the various influences affect snow cover and low-elevation ice sheets in regions of the northern hemisphere where ice existed at the Last Glacial Maximum (LGM). As we show, the GCM is generally incapable of simulating the beginnings of ice sheet growth, or of maintaining low-elevation ice sheets, regardless of the orbital parameters or sea surface temperatures used. The discrepancy is examined in light of its implications for climate model sensitivity and orbital parameter initiation of ice sheet growth.

2. MODEL

The experiments use the GISS GCM run at $8^\circ \times 10^\circ$ (latitude by longitude) horizontal resolution, with nine layers in the vertical [*Hansen et al., 1983*]. The model numerically solves the primitive equations for the conservation of energy, mass, and momentum, as well as conservation of moisture. It uses realistic topography averaged over the model grid box for both dynamical and thermodynamic calculations, with each grid box containing the appropriate fraction of land, water, ocean ice, and land ice. We discuss here aspects of the model that are particularly important for the current studies.

The model calculates the thermal and solar radiative fluxes, including a diurnal cycle. Cloud cover is calculated, with the cloud albedo a function of altitude and temperature, as

$$\begin{aligned} T > 258 \text{ K} \quad \tau &= 0.0133[p(\text{mbar}) - 100] \\ T < 258 \text{ K} \quad \tau &= 1/3 \end{aligned} \quad (1)$$

with τ the optical thickness; low-altitude clouds have the largest albedos, and cirrus clouds the smallest.

The model calculates snow cover as the balance of snowfall, melting, and sublimation. Snowfall occurs as a form of large-scale precipitation. Under supersaturated conditions, moisture is condensed to reduce the relative humidity of one of the nine layers to 100%; the moisture can be reevaporated in any lower layer that is unsaturated, and if the temperature of the lowest model layer (at a mean pressure of 959 mbar) is below freezing, the precipitation is in the form of snow.

The model contains two ground layers; if the temperature of the upper layer, with a depth of 10 cm, is less than or equal to 0°C , the snow depth increases. Otherwise, the snow melts, decreasing the ground temperature. Net heating of a snow surface raises the ground temperature as high as 0°C , and additional heating causes snow melting, which occurs uniformly throughout the grid box. Snowmelt goes into runoff or ground moisture, depending on the rate of melting and the ground wetness:

$$R = \frac{1}{2}W_1S_m \quad (2)$$

where R is runoff, S_m the snowmelt rate, and W_1 the first-layer ground wetness, defined as the ratio of moisture present to the total moisture-holding capacity of the ground (a function of vegetation type, as given by *Hansen et al. [1983]*).

Sublimation can occur with sufficient surface heating and net evaporation, as determined by

$$E = \beta E_p \quad (3)$$

where E is net evaporation, β is an efficiency factor set equal to the first-layer ground wetness W_1 , and E_p is the potential evaporation of a wet surface. This latter quantity is determined energetically as the flux of latent heat:

$$F_q = pC_qV_s(q_g - q_s) \quad (4)$$

with V_s the surface wind velocity, q_s the surface air specific humidity, and q_g the saturated moisture value right above the ground. C_q , the moisture transfer coefficient, is set equal to the heat transfer coefficient, which is a function of the surface roughness and the atmospheric stability as defined in terms of the Richardson number (see *Hansen et al. [1983]* for the complete formulation). The transfer coefficients maximize when the atmosphere is unstable, i.e., the ground temperature is warmer than the atmospheric temperature, and are smallest when the temperature gradient is negative (temperature increasing with altitude above the ground).

The spectrally weighted albedo of snow-covered ground varies with snow depth and melting age, vegetation cover, and the albedo of the underlying ground:

$$A = A_g + (A_s - A_g)[1 - \exp(-d_s/d_s^*)] \quad (5)$$

where A is the albedo of the snow-covered ground, A_g the albedo of the snow-free ground, A_s the snow albedo for infinite depth, and d_s and d_s^* the snow depth and masking depth in equivalent thickness of liquid water. The masking depth is associated in the model with the vegetation types in a particular area, and it varies from 1 cm of water in the tundra regions to 90 cm of water in thickly forested regions. The snow albedo varies as a function of snow age as

$$A_s = 0.5 + 0.35(\exp - a_s/5) \quad (6)$$

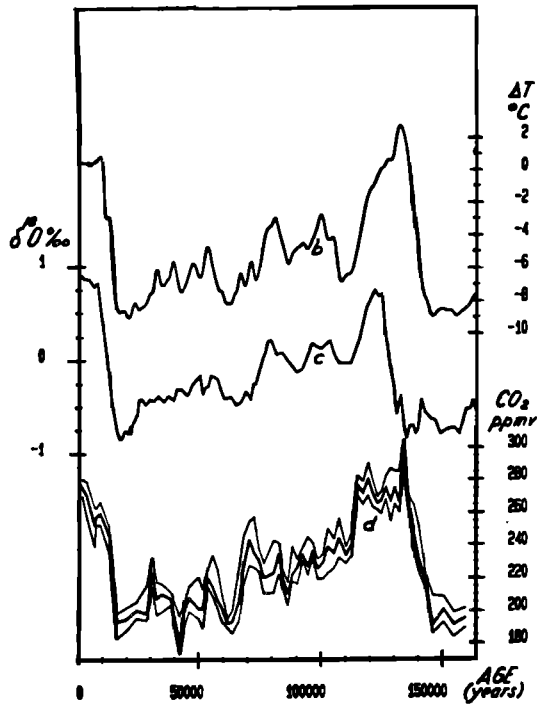


Fig. 3. Vostok isotopic temperature difference from today (curve *b*), marine benthic $\delta^{18}\text{O}$ (curve *c*), and Vostok CO_2 concentrations, showing the best estimate (heavy line) and uncertainties (curve *d*) [after *Lorius et al.*, 1988]

where a_s is the age of the upper snow layer in days, computed from

$$a_s(t + \Delta t) = \{a_s(t) + [1 - a_s(t)/a_0]\Delta t\} \exp(-\Delta d_s/d_s) \quad (7)$$

Here Δd_s is the snowfall in time Δt , d_s is the depth required to refresh the snow albedo, taken as 0.2 cm, and a_0 is an old age limit taken as 50 days. Thus fresh snow has an albedo of 0.85, and old snow 0.50. With this prescription, the surface albedos in snow-covered regions in the current climate control run compared well with observations [*Hansen et al.*, 1983].

The snow-free albedo of land ice is the same as for aged snow: 0.6 in the visible, 0.35 in the near IR, and 0.5 spectrally weighted. The model includes land ice as a fixed boundary condition and thus will not remove it or lower its altitude. As land ice melts, more land ice is "pushed up from below" to maintain the constant altitude, with the amount necessary recorded in the diagnostics.

The sea surface temperatures in the model can be specified or can be generated directly. In the generation mode, the monthly mixed layer depths and ocean transports are prescribed in such a fashion that the calculated temperatures reproduce the observed temperatures for the model's cur-

rent climate simulation [*Hansen et al.*, 1984]. We use both versions in the experiments described below. When the sea surface temperatures are calculated, sea ice forms when the temperatures drop below -1.6°C . The details of the sea ice formation and its associated thickness, albedo, etc., are described by *Hansen et al.* [1983, 1984].

3. EXPERIMENTS

Shown in Figure 3 is the smoothed deuterium isotopic temperature record determined from the Vostok ice core, and a marine North Atlantic benthic $\delta^{18}\text{O}$ record, suggestive of global continental ice volume changes. Rapid cooling and ice sheet growth appear to have set in around 120 kyr B.P. and to last to about 100–110 kyr B.P. (see also *Barnola et al.* [1987]). The Vostok temperature at the peak of the LGM, 15–20 kyr B.P. was only slightly colder than the minimum temperatures indicated at 110 kyr B.P. The ice volume as reflected in the ocean isotopic record was less at 110 kyr B.P. than during the glacial maximum, but is about 1/2 of the glacial-interglacial drop, a substantial volume. *Kukla* [1980] estimated from pollen records that the initiation of the last glaciation in Europe occurred about 115 kyr B.P. The timing of these records has uncertainties, and the translation of isotope changes to ice volume changes is complicated by part of the signal which represents ocean temperature changes; nevertheless, the solar radiation record for this time period indicates sharp reductions in summertime insolation at northern latitudes, consistent with what one would expect as a condition for ice growth.

We thus performed a series of experiments using the GISS GCM to simulate the climate of time periods corresponding to the orbital configuration of 116 kyr B.P., when July insolation was near its minimum value at 60°N , at 106 kyr B.P., when September insolation was relatively small, and a modified insolation field (MIF), which greatly exaggerated the changes occurring in the insolation distribution between 116 and 114 kyr B.P. The time 116 kyr B.P. was chosen because ice appears to have been increasing rapidly then (Figure 3). The 106 kyr B.P. experiment was chosen as a time when this stadial grew to its peak volume. The MIF input was used in an attempt to greatly augment the insolation forcing at the climatic transition and reveal which feedbacks in the system could be supported by the insolation shift.

The orbital parameters used in the three cases and the control run are presented in Table 1, where ω is the angle from the vernal equinox to perihelion in radians. The MIF was obtained by determining the insolation change from 116 to 114 kyr B.P. (when ice was apparently growing rapidly), multiplying this difference by a factor of 5, and then fitting the results as closely as possible with a new set of orbital parameters. We are thus exaggerating the tendency

TABLE 1. Orbital Parameters in the Different Experiments

Run	Obliquity	Eccentricity	Omega	Perihelion, Days From Jan. 1
0 kyr	23.44	0.01670	4.938	1.8
116 kyr B.P.	22.48	0.04141	-1.482	-4.7
106 kyr B.P.	22.82	0.04037	-4.858	-205.5
Modified	22.00	0.10900	0.045	81.3

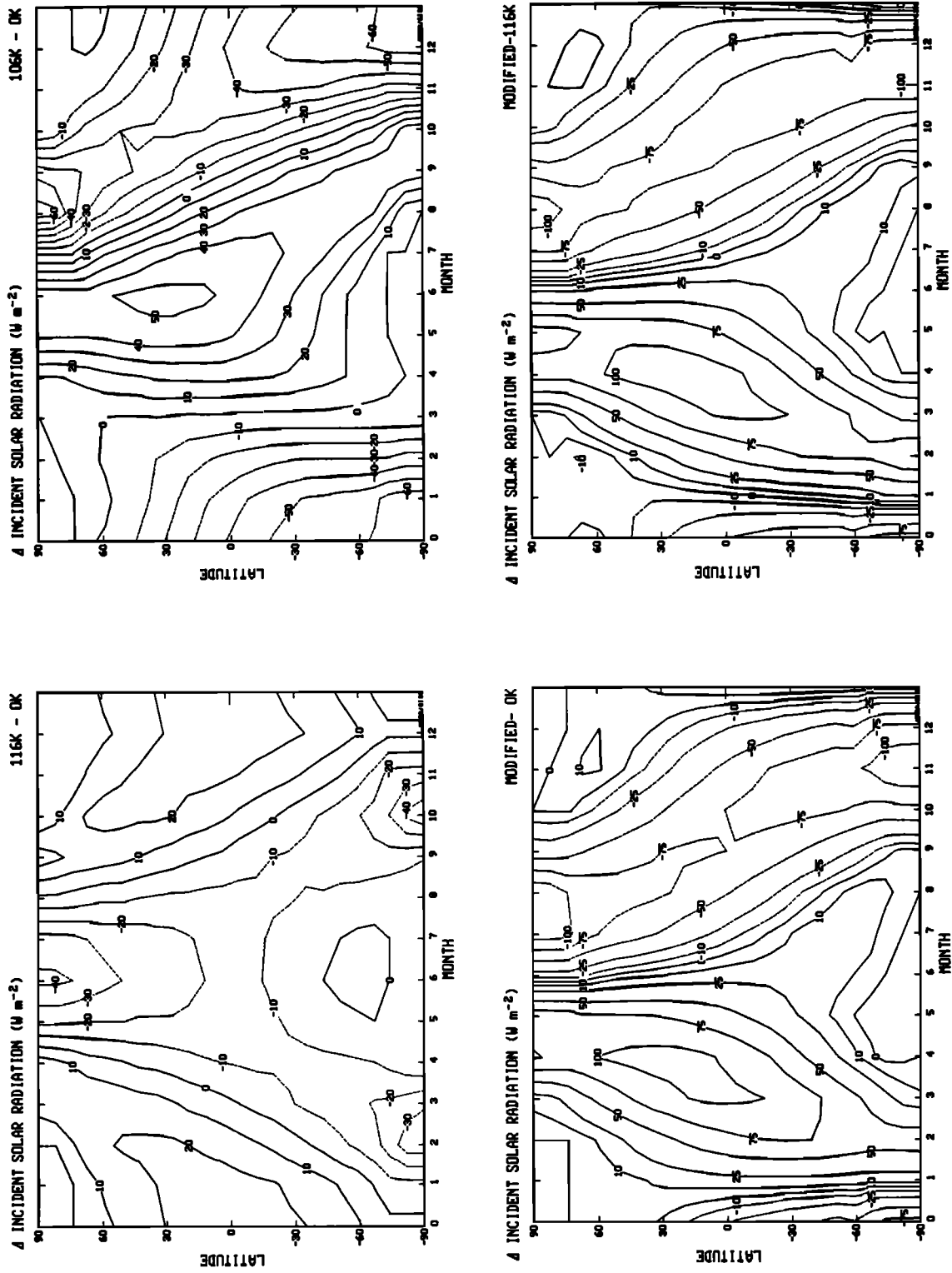


Fig. 4. Change in incident solar radiation as a function of month between (top left) 116 kyr B.P. and today, (top right) 106 kyr B.P. and today, (bottom left) modified incident radiation (MIR) and today, and (bottom right) the MIR and 116 kyr B.P.

TABLE 2. Description of Experiments

Run	Conditions
Current	Current climate, with current orbital parameters and SSTs
Con 1	116 kyr B.P. orbital parameters and current SSTs
Exp 1	Modified orbital parameters and current SSTs
Con 2	116 kyr B.P. orbital parameters and calculated SSTs
Exp 2	Modified orbital parameters and calculated SSTs
Exp 3	Exp 2 with 10-m land ice in locations of 18-kyr land ice
Exp 4	Exp 3 with carbon dioxide reduced by 70 ppm
Exp 5	Exp 3 with actual 106 kyr B.P. orbital parameters
Exp 6	Exp 4 with CLIMAP 18 kyr SSTs and sea ice
Exp 7	Exp 4 with (CLIMAP minus 2°C) SSTs and sea ice

SSTs, sea surface temperatures.

that was evident when the geophysical evidence implies ice sheet growth was favored. The resulting differences in incident solar radiation between 116 kyr B.P., 106 kyr B.P., and the MIF with today's values are shown in Figure 4. At 116 kyr B.P., early summer solar radiation was reduced by 4–8% at extratropical latitudes in the northern hemisphere (Figure 4, top left). By 106 kyr B.P., incident radiation had increased at these latitudes during the first half of summer, but it decreased by about 10% during the second half (Figure 4, top right). The MIF run amplified the reductions to peak values close to 25% and extended the deficit throughout the summer season (Figure 4, bottom left). As shown by the comparison between the MIF and 116 kyr B.P. values (Figure 4, bottom right) (the solar insolation tendency occurring from 116 to 114 kyr B.P. provided for reduced insolation during late summer and fall

As discussed by *Kutzbach and Gallimore* [1988], ambiguities arise when discussing specific months for cases with different orbital parameters. For example, if the northern hemisphere summer solstice starts on a different day as the orbital parameters are changed, then comparisons of the month of June will include more or less of summer in the different situations. We avoid this problem in these experiments by defining the months relative to a fixed vernal equinox.

Experiments with the different orbital parameters were run with both specified sea surface temperatures, and with sea surface temperatures allowed to vary. In addition, various other parameters were changed as the experiments proceeded. The aim in all cases was to investigate whether the more favorable solar radiation would have allowed ice sheets to develop or grow in the GCM. The individual experiments are presented in Table 2. A specific description of the different experiments is presented in the next section, along with the results. Each experiment was run for 3 years, integrating through the annual cycle, following a 1 year spin-up. Several additional experiments were made to test model sensitivities; they are presented in the discussion section.

4. RESULTS

4.1. Specified Sea Surface Temperature Experiments

The 116 kyr B.P. experiment (called Con 1 in Table 2, as it serves as a control run for the first set of experiments) was run with the sea surface temperatures specified at today's

values. This limits the air temperature changes over the ocean and results in temperature changes over land being in phase with solar radiation changes. As evident in Figure 4, the solar radiation differences between 116 kyr B.P. and today feature reduced insolation during summer at high northern latitudes, with increases in the other seasons. Thus as expected, the temperature changes between 116 kyr B.P. and model values for the current climate (see Table 2) have this same seasonal variation, shown in Figure 5. (As our interest is in ice sheet growth in the northern hemisphere, we show in this and the following figures only results poleward of 30°N.)

The temperature decreases in summer are not large, compared with the estimates of the cooling needed for ice initiation to take place. The cooling is slightly less than that produced by *Royer et al.* [1984] in a 1-year simulation for 115

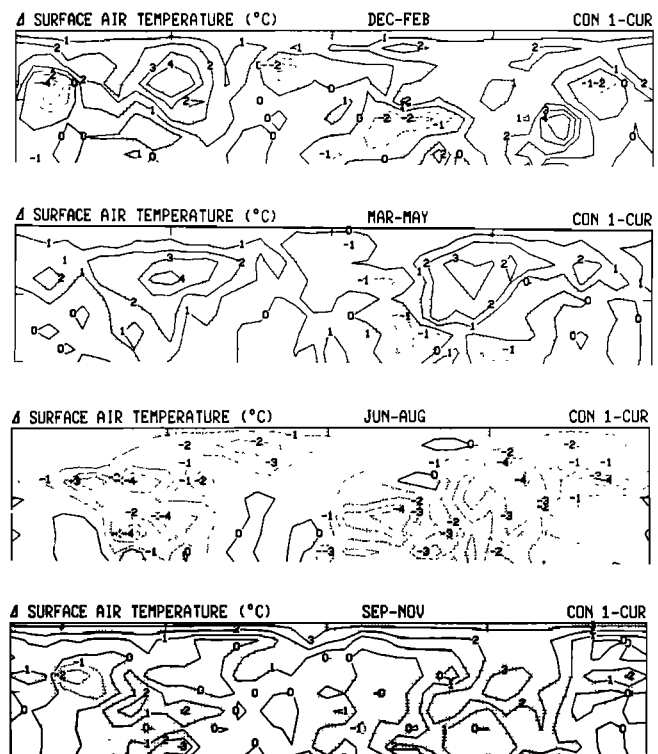


Fig. 5. Temperature change between 116 kyr B.P., with current sea surface temperatures, and today for different seasons, the difference between control run 1 and the current climate simulation.

kyr B.P. A necessary ingredient for ice sheets to grow is the ability to have snow last through the summer season. Shown in Figure 6 is the model's distribution of snow depths in July for several of the experiments and control runs. At 116 kyr B.P., snow cover occurs at times during the month in the Keewatin District of the Northwest Territories. It does not, however, last continually through the month (generally true for values less than 1-cm snow depth). The 116 kyr B.P. experiment with sea surface temperatures specified at current values could not have initiated ice sheet growth in this GCM.

What about the situation with the more extreme summer radiation deficit? Given the difficulty which the model has for 116 kyr B.P. in maintaining snow cover through the summer, we use the MIF, again with the current specified sea surface temperatures (with this experiment referred to as Exp 1 in Table 2). Relative to 116 kyr B.P., the solar radiation in this experiment is increased in spring and early summer and reduced from late summer through winter (Figure 4). The surface air temperature differences follow a similar trend. In particular, as shown in Figure 7, temperatures at upper mid-latitudes warm in June, show little change in July, and cool in August and September. With this pattern of temperature change, showing little additional cooling in mid-summer, there is still no tendency for snow to persist through July (Figure 6).

4.2. Effect of Varying Sea Surface Temperatures

One major drawback of the former experiments is in the specification of the sea surface temperatures. As the seasonal insolation is somewhat different from today, there is no reason for the sea surface temperatures to be the same as

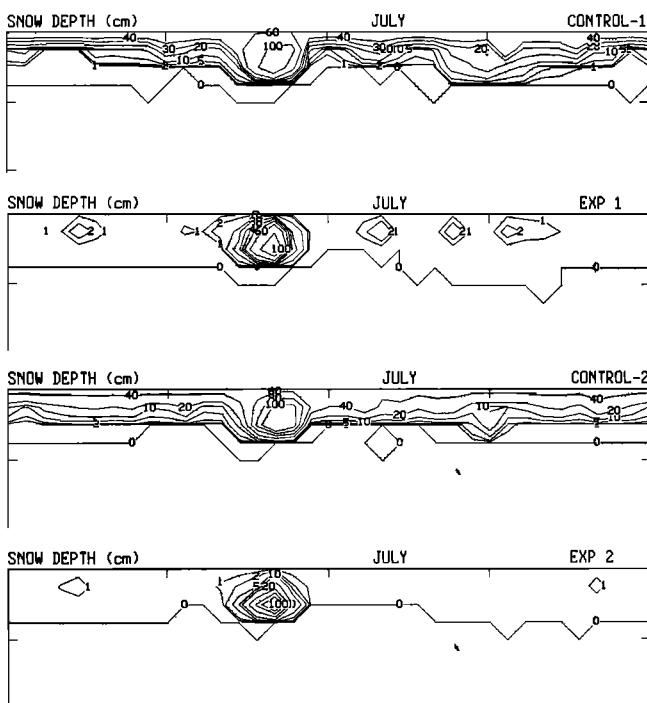


Fig. 6. Snow depth during July for different model runs. Values less than 1 cm generally indicate snow cover is not continuous during the month.

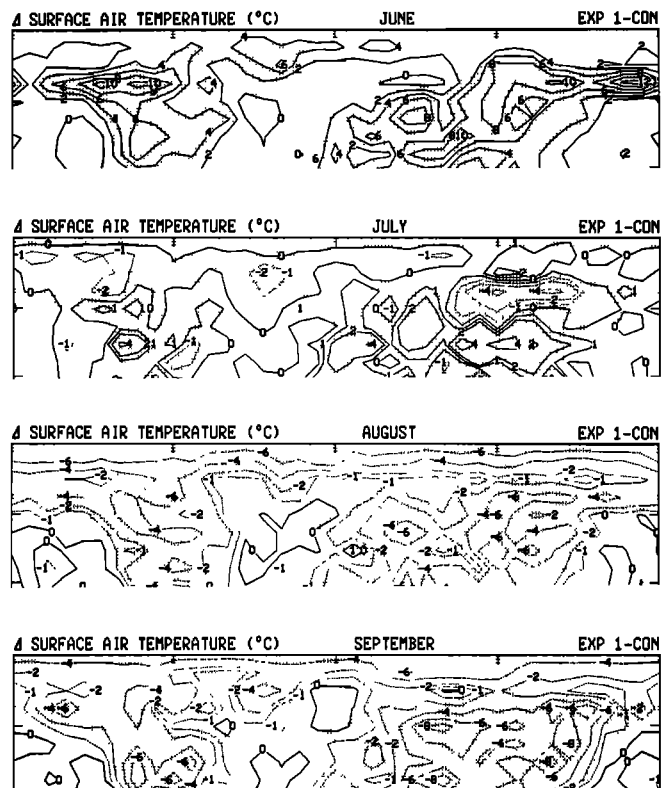


Fig. 7. Monthly temperature differences during summer between experiment 1, with the MIR and sea surface temperatures specified at current values, and its control for 116 kyr B.P.

current values. In the following experiments, we allow the sea surface temperatures to change while keeping the ocean heat transports fixed at the values used in the current climate runs [Hansen et al., 1984]. While the transports themselves may have changed if wind velocities and deep-water formation were altered, keeping them fixed represents a higher order assumption than specifying the temperatures. As shown, we subsequently (implicitly) drop this assumption as well.

One other difficulty arises in experiments in which the sea surface temperatures are allowed to adjust: for the ocean to come into equilibrium with the altered solar forcing would require 30-year experiments. As the following runs were for only 4 years, we obviously do not reproduce equilibrium results. However, we can estimate the amount of adjustment that would have resulted during the additional integration time by noting the net radiation at the top of the atmosphere. In the doubled CO_2 experiments, a 4 W m^{-2} imbalance in this diagnostic is eventually converted by the GCM into a 4.2°C warming, establishing a model sensitivity of about 1°C for a 1 W m^{-2} imbalance. This sensitivity holds true ($\pm 20\%$) with a variety of climate forcings of both warming and cooling. We can thus estimate the equilibrium temperature change which would have resulted, at least on a global basis, from the modeled imbalance during the few years of these experiments. In the final experiments, we cool the ocean to values consistent with this imbalance.

We first repeat the two previous experiments, for 116 kyr B.P. (Con 2) and the MIF (experiment 2). In comparison with the results in the specified sea surface temperature runs, the excess solar radiation in spring leads to warmer

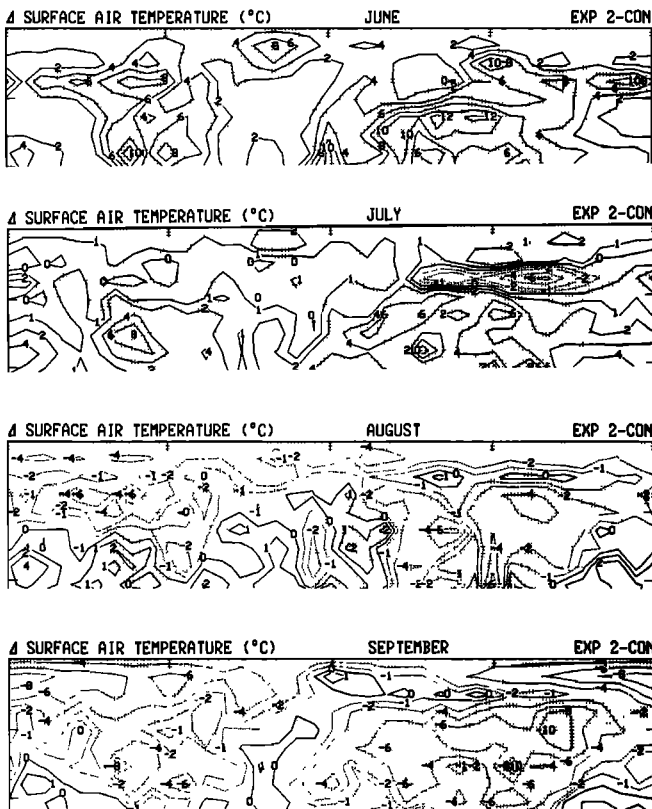


Fig. 8. As in Figure 7 except for experiment 2, with the MIR and varying sea surface temperatures, minus its control with 116 kyr B.P. radiation.

ocean and land temperatures in spring and summer, while the reduced radiation in late summer leads to cooler temperatures in fall. Allowing the sea surface temperatures to change thus magnifies the influence of the radiation imbalance and extends its effect into the subsequent season. In the particular regions of interest, comparison of the results from this experiment minus its control run (Figure 8) with those shown in Figure 7 indicates little in the way of substantial differences. Thus, as shown in Figure 6, neither the experiment nor the control run with varying sea surface temperatures maintains additional snow cover through July.

If run to equilibrium, would the results have been any different? The model simulation for the current climate has a net radiative imbalance at the top of the atmosphere of about 7.5 W m^{-2} [Hansen et al., 1984], of which close to 2.5 W

m^{-2} is due to computer truncation (IBM and compatible machines truncate rather than rounding off) and loss of kinetic energy to friction by surface drag (which is not then reconverted into heat). The excess 5 W m^{-2} is absorbed by the ocean and ocean ice, and is presumably due to inaccuracies in cloud properties, surface albedo, thermal emission calculations, etc. If experiments which allow the sea surface temperatures to change use this excess radiative energy, the ocean temperatures would warm spuriously. Thus in the varying sea surface temperature experiments, the solar radiation absorbed at the ocean's surface is multiplied by a factor of 0.96, which brings the current climate simulation into radiative equilibrium and removes any bias in the other runs. The procedure does not, however, guarantee equilibrium in the changed climate experiments.

Presented in Table 3 are the global, annual average net radiative imbalances at the top of the atmosphere relative to the value for the current climate for the various experiments. Shown are the changes in incident solar radiation per unit area S_0 , in the planetary albedo A , and in the solar radiation absorbed below the top of the atmosphere (incident energy minus reflected); also shown are the changes in the ground temperature (T_g), the atmospheric transmissivity (greater transmissivity implies less greenhouse capacity of the atmosphere), defined as $\tau = S_0(1 - A)/(\sigma T_g^4)$, with σ the Stephan-Boltzman constant, and the change in the net long wave emission, due to terrestrial radiation. The change in the energy balance, representing the sum of the changes in the short wave absorption and long wave emission, is given in the last column. Note that for all the experiments the change in the global, annual average incoming short wave energy is quite small, and the change in short wave absorption is usually associated mostly with the planetary albedo change (increased albedo leading to reduced absorption). The change in the long wave emission (with negative values meaning a greater outward flux) is associated with the change in temperature or transmissivity changes due to altered CO_2 , water vapor, and clouds.

Con 2 for 116 kyr B.P. has a small radiation imbalance which, given the model sensitivity noted above, implies it would have cooled by about 0.5°C globally, had the model been run to equilibrium. The results shown above are averages for years 2–4. During year 4, the imbalance had been reduced by gradual cooling, so that the remaining cooling would have only been 0.3°C . Comparison of year 4 with the 3-year average failed to show any obvious differences. Given these results, and the small values of the

TABLE 3. Radiative Balance (at Model Top) Compared With Current Climate

Run	Short Wave Incident, W m^{-2}	Planetary Albedo, %	Short Wave Absorbed, W m^{-2}	T_g , $^\circ\text{C}$	τ	Long Wave Emission, W m^{-2}	Balance, W m^{-2}
Current	342.3	30.24	240.5	15.5	0.61	-233.0	7.5
$\Delta\text{Con 1}$	-0.2	-0.53	-0.1	-0.2	0.01	0.4	0.3
$\Delta\text{Exp 1}$	1.6	-0.47	1.0	0.0	0.01	-0.6	0.4
$\Delta\text{Con 2}$	-0.2	-0.34	-0.7	-0.2	0.00	0.1	-0.6
$\Delta\text{Exp 2}$	1.6	-0.53	1.2	0.4	0.00	-1.4	-0.2
$\Delta\text{Exp 3}$	1.6	0.07	-0.9	-0.7	0.01	0.6	-0.3
$\Delta\text{Exp 4}$	1.6	0.05	-0.8	-0.7	0.01	-1.7	-2.4
$\Delta\text{Exp 5}$	-0.2	0.11	-2.3	-1.0	0.01	1.6	-0.6
$\Delta\text{Exp 6}$	1.6	1.12	-4.4	-3.2	0.02	1.6	-2.9
$\Delta\text{Exp 7}$	1.6	1.54	-5.9	-5.2	0.04	5.8	-0.2

imbalance, it does not appear as if the results would have been much different had this experiment been integrated further.

This conclusion is even more true for experiment 2, with the MIF radiation field. As shown in Table 3, the model with these radiation conditions is already in approximate equilibrium, at least from the annual and global perspective. Again, comparison of year 4 with the 3-year average failed to indicate any substantive differences.

4.3. Effect of 10-m-Thick Land Ice

While the preceding experiments failed to maintain snow cover through July, and thus would not have been able to build ice sheets, they did not march through the range of orbital variations which the real climate system experienced en route to generating ice sheets. Perhaps some other orbital parameter configuration could have initiated the ice sheet, and all that would have been required in the experiments conducted here would be for the ice sheet to grow. If this were the case, once the ice sheet was in place, it conceivably could have altered the local or global climate in such a way as to maintain its existence. Furthermore, the coarse model resolution could not be expected to properly simulate isolated snow cover areas on higher terrain or in shaded regions, which perhaps could have then spread over surrounding regions. Nor does the model have glacial dynamics, which might allow ice to grow at some very high latitude and spread southward, where it would then influence the climate and provide for more favorable growth conditions.

To investigate these possibilities, the next series of experiments incorporated 10-m-thick ice sheets already in place. The attempt was then to determine whether the model would have maintained the ice sheet on an annual basis. As indicated in the introduction, there is some uncertainty as to where the ice sheets really began; if the initial ice sheet were put in the “wrong place,” the ability of the model to maintain it would not provide an adequate assessment of the effectiveness of orbital parameter variations.

Thus to ensure optimum conditions for ice sheet growth, we input 10-m-thick ice into all locations where land ice was found during the LGM, as indicated in the *CLIMAP Project Members* [1981] data set; Figure 2 indicates the area covered with ice over North America. (An exception was made in the case of Hudson Bay, which was allowed to generate its own sea surface temperatures and sea ice in the next few experiments, but kept very cold in the final two experiments; as indicated in the discussion section, this choice does not dominate the results.) The widespread location of the ice also allows air being advected into high-latitude regions to be cooled prior to affecting prospective source regions. We will investigate the fate of these low-elevation ice sheets from both an energy and a mass balance perspective.

Experiment 3 was then similar to experiment 2 with the inclusion of 10 m of ice. Shown in Figure 9 are the surface air temperatures relative to the model run for the current climate. Substantial cooling occurs in the vicinity of the ice sheets in all four seasons, with values during summer of a magnitude similar to those estimated as being necessary to initiate ice sheet growth. The large magnitudes of cooling in summer and fall are associated with reduced solar insolation absorption (Figure 10), due to reduced insolation (Figure 4) as well as higher surface albedo and increased (basically low

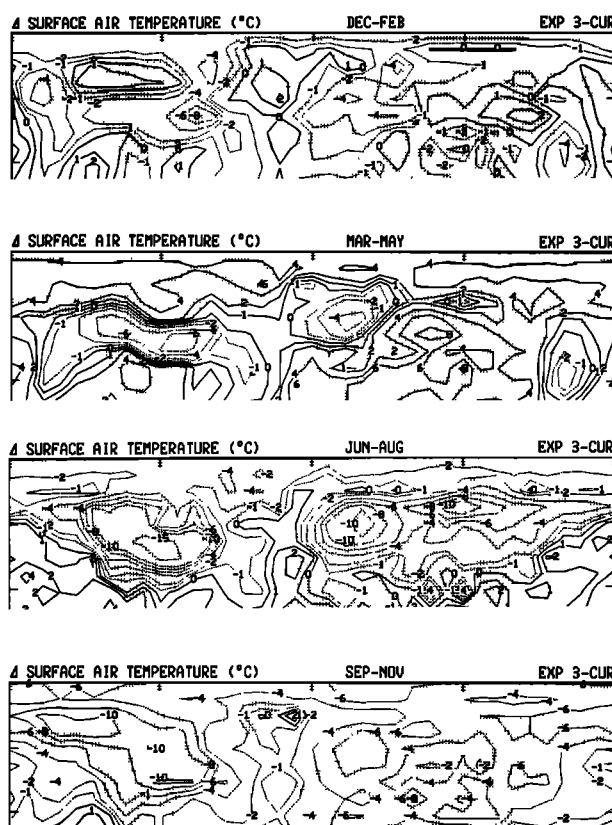


Fig. 9. Seasonal temperature differences between experiment 3, with 10-m land ice and MIR, and the model's current climate simulation.

level) cloud cover (Figure 10), with low clouds forming over the ice sheets. In addition, the presence of the ice keeps the surface air temperature near freezing, as any additional heat goes into melting the ice. The total net radiation charge at the surface (Figure 10) is not as negative as the net solar radiation charge, for the colder temperatures limit long wave radiation out to space. And the total net heating charge at the surface during this season is actually positive south of Hudson Bay and over Eurasia (Figure 10), despite the reduced solar absorption, for the colder surface has greatly reduced sensible and latent heat fluxes due to the greater atmospheric stability induced by the cold ice surface.

The absolute values of the energy balance in the vicinity of the ice sheets are shown in Figure 11. The net radiation, although greatly reduced, is still strongly positive, despite the presence of some 70% cloud cover. The sensible heat flux is causing the surface to lose energy, but this value is also reduced, by some 20 W m^{-2} compared with model current climate values in these regions. The net heating at the surface is approximately $10\text{--}20 \text{ W m}^{-2}$ in most of the areas suggested as being responsible for initiating ice sheet growth.

To put this value in perspective, consider that a volume of ice with an area of 1 m^2 , an altitude of 10 m, and a density of 0.917 g cm^{-3} has a total mass of $9.17 \times 10^6 \text{ g}$. The total heat needed to melt this ice, given that it takes 334.88 J to melt 1 g of ice, is then $3.07 \times 10^9 \text{ J}$, or approximately $3.55 \times 10^4 \text{ W days}$. So for the same 1-m^2 area, a heating imbalance of 20 W would take 1774.5 days, or 4.86 years to melt the 10 m of ice.

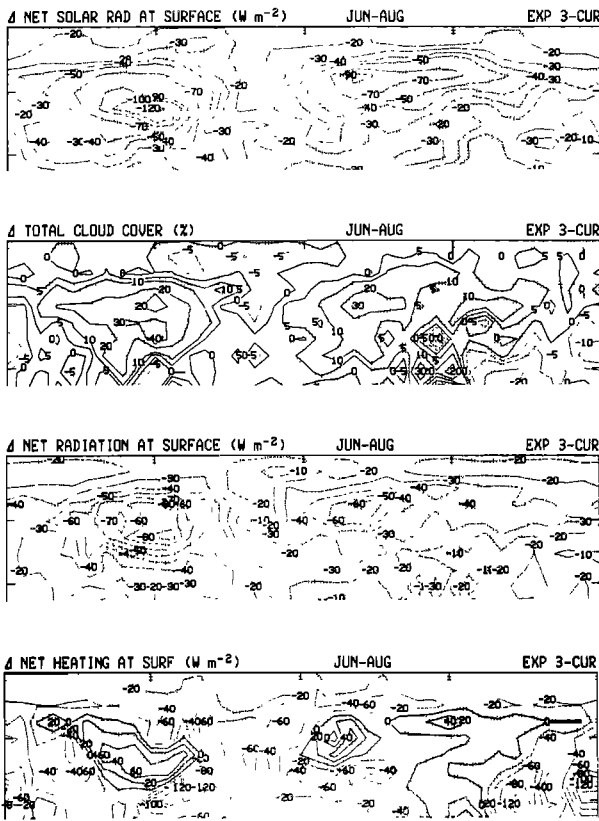


Fig. 10 Change in net solar radiation absorbed at the surface, total cloud cover, net radiation at the surface, experiment 3 minus model current climate, for June-August

In the model the ice does not disappear, as more is pushed up from below. Nevertheless it would have disappeared, and rapidly, were it allowed to. Furthermore, the melting that was going on forced the surface air temperature to remain near the freezing value, and was instrumental in producing the large surface air temperature depression seen in Figure 9. Were the ice allowed to melt completely away, the excess heat would have increased the surface air temperature to values more like those of experiment 2.

The same conclusion can be reached by considering the mass balance. The presence of the ice and the associated colder temperatures builds higher sea level pressure in most seasons, as shown by the results for summer (Figure 12). The relative wind flow around this high-pressure region advects moisture northward over the central Hudson Bay area. The cold surface high becomes a trough above by 500 mbar, and the resulting upper air flow produces relative south to north winds from Hudson Bay eastward. The result is to produce increased rainfall in a narrow region in the vicinity of Hudson Bay, while the higher pressure reduces rainfall elsewhere in the vicinity.

The absolute value of the annual mass balance components, precipitation, evaporation and runoff, are shown in Figure 13. Precipitation values in the regions of interest are of the order of 1.5 mm d⁻¹. Evaporation over land ice is approximately 0.25 mm d⁻¹. The surface runoff, due primarily to ice melting, is 5–10 mm d⁻¹. The net negative imbalance of approximately 6 mm d⁻¹ would cause the 10-m-thick ice sheets to disappear in 1667 days, or approx-

imately 4.6 years, consistent with the energy balance calculation.

The energy and mass balances are not independent, since the excess energy is responsible for ice melt and runoff, and it is this term which is making the mass balance negative (precipitation exceeds evaporation over the land ice). Furthermore, neither gives a completely accurate representation of the ice disappearance; the annual net surface heating includes a negative energy balance during winter, which would not compensate for the positive balance and melting during summer, and the precipitation might be rain, which would not help ice sheet growth. The similarity in disappearance times calculated by the two techniques implies that these effects are not dominating their respective balances. However, a more accurate appraisal of the fate of the ice sheets is the monthly distribution of the actual melting rates for land ice at several different latitudes given in Table 4. The extreme nature of the imbalance is emphasized by noting that in this experiment (experiment 3) the 10 m of ice for the latitudes as a whole would have disappeared in about 4 years.

Reference to Table 3 shows that the net radiation imbalance at the top of the atmosphere is small in experiment 3, as the slight increase in planetary albedo due to the land ice leads to reduced short wave absorption, while the colder ground temperatures lead to reduced long wave emission. Thus this run is also in approximate radiation equilibrium. Again, comparison of year 4 to the 3-year average failed to indicate any changes in results. Both of these factors imply that further integration would not have altered the basic conclusions.

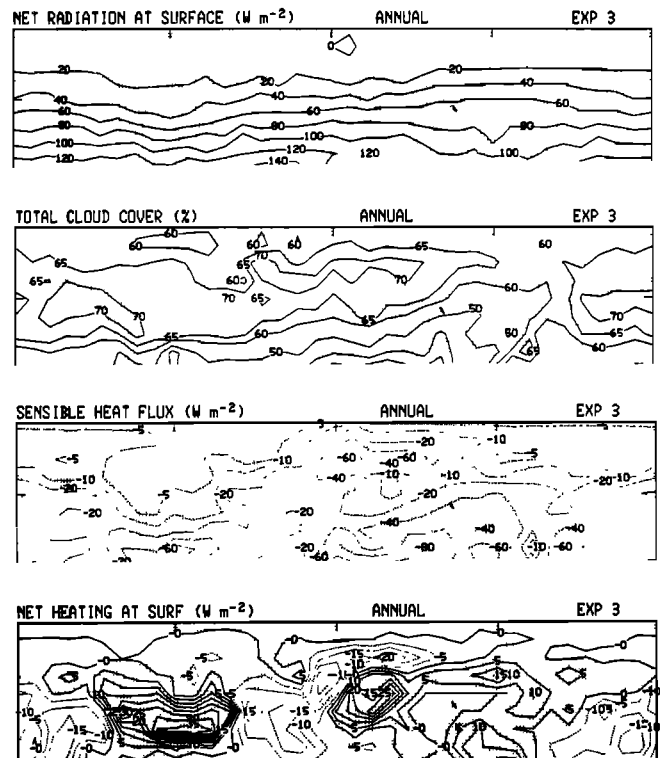


Fig. 11. Annual average net radiation absorbed at the surface, total cloud cover, sensible heat flux, and net heating at the surface in experiment 3.

4.4. *Effect of Reduced Carbon Dioxide*

Observations of the CO₂ levels in the Vostok ice core show reduced values of up to 70 ppm (e.g., 300–230 ppm) were possible during the 116–106 kyr B.P. interval (Figure 3). In experiment 4 we thus reduced the atmospheric CO₂ by this amount. The run was not integrated sufficiently to allow the full magnitude of the effect to become apparent, and thus surface air temperatures cooled only slightly relative to experiment 3 (Figure 14). The reduced CO₂ did result in increased thermal energy loss from the surface, and both the net radiation and net heating were reduced by a few W m⁻². This magnitude of change does not produce a noticeable effect on ice melting rates, as shown by the value of the net surface heating (Figure 14). But the impact of the full effect may be deduced by reference to the net radiation imbalance at the top of the atmosphere of 2.4 W m⁻² (Table 3), associated with slightly increased transmissivity and long wave emissions. Substantial cooling of the order of 2.5°C would have resulted if this run had been continued to equilibrium. Furthermore, the large negative heating over

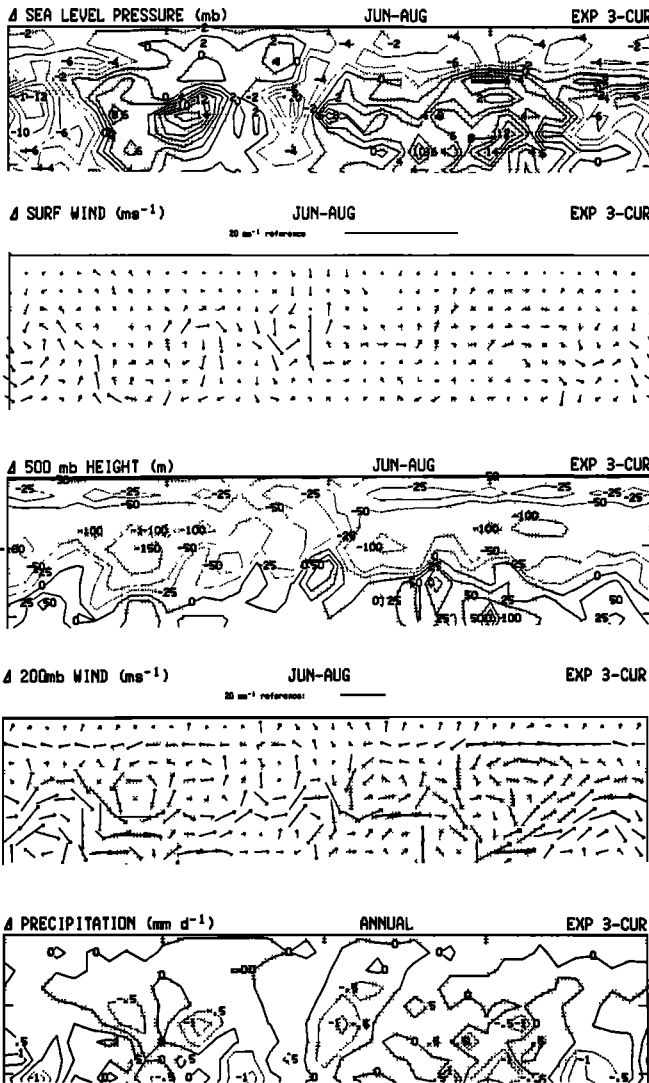


Fig. 12. Change of sea level pressure, surface wind, 500-mbar height, and 200-mbar wind for June–August, along with annual precipitation change, for experiment 3 minus model current climate.

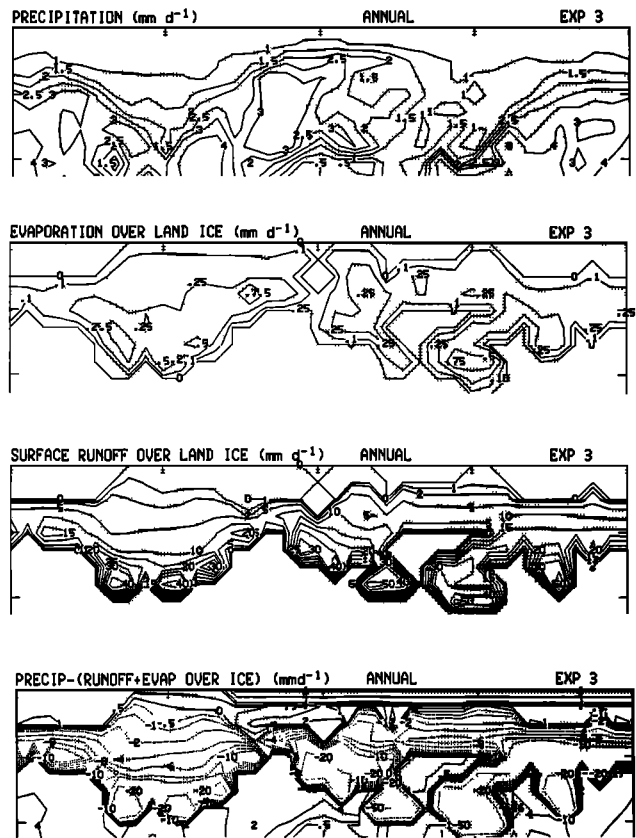


Fig. 13. Annual average precipitation, evaporation over land ice, surface runoff over land ice, and total mass balance over land ice in experiment 3.

the ocean surface (Figure 14, bottom) implies that the North Atlantic in particular would have gotten cooler. We investigate this more closely below, in experiment 6.

4.5. *Effect of Actual 106 kyr B.P. Radiation*

The experiments so far have used either the 116 kyr B.P. orbital parameters, or the “modified” insolation values. How sensitive are the results to the particular specification? As shown in Figure 3, the MIF radiation has reduced solar insolation at extratropical northern latitudes in late summer, but increased insolation values in spring. In both experiments 3 and 4 the melting is greatest in May and June (see Table 4), so it is natural to inquire whether the actual 106 kyr B.P. radiation, with relatively smaller values in these months, would provide better conditions for sustaining the ice. Thus in experiment 5 we use the real 106 kyr B.P. radiation values. In all other respects, experiments 3 and 5 are similar. The melting rates for experiment 5 (Table 4) indicate that the most rapid melting shifts to the summer months, but the total annual melting is very similar. This is an important result, for it implies that the model is not capable of sustaining the ice under the conditions of these experiments with a range of orbital parameters. It furthermore implies that were the model to be run for thousands of years, with orbital parameters slowly changing, the results might not be any different. Notice again that in Table 4, the 10 m of land ice, on a latitudinal average, melts in about 3 years. The small radiation imbalance (Table 3), similar to

TABLE 4. Zonal Average Ice Sheet Balance (mm d^{-1})

Experiment	Jan.	Feb.	March	April	May	June	July	Aug.	Sept.	Oct.	Nov.	Dec.	Annual Melt, m/yr
<i>63°–71°N</i>													
3	0.7	1.1	0.7	-1.3	-16.3	-18.1	-15.8	-5.4	-1.1	0.0	0.4	0.4	1.5
5	0.9	1.1	0.9	-0.4	-6.7	-18.1	-19.9	-11.6	-1.8	0.0	0.2	0.4	1.9
6	0.7	0.9	0.9	0.2	-6.3	-14.1	-6.7	-1.3	0.0	0.2	0.5	0.4	0.7
7	0.7	0.5	0.5	0.4	-3.1	-9.2	-5.2	-0.7	0.0	0.2	0.5	0.5	0.4
<i>55°–63°N</i>													
3	0.8	1.2	0.8	-1.4	-20.5	-23.0	-17.9	-11.9	-4.8	-0.7	-0.2	0.0	2.5
5	0.4	0.8	-0.4	-4.3	-13.6	-19.6	-20.6	-18.0	-7.8	-1.0	-0.2	0.0	3.1
6	0.6	1.2	0.6	-3.3	-15.6	-18.3	-13.2	-5.8	-2.1	-0.6	0.0	0.2	1.7
7	0.8	0.6	0.6	-2.7	-13.7	-16.0	-10.2	-3.3	-1.4	-0.2	0.0	0.4	1.1
<i>47°–55°N</i>													
3	-0.5	-0.5	-5.9	-18.0	-27.0	-27.0	-23.9	-14.7	-8.2	-2.6	-0.5	-0.8	3.6
5	-0.8	-0.5	-1.8	-12.1	-21.9	-26.2	-27.8	-24.4	-12.3	-2.6	-1.0	-0.8	4.2
6	0.0	0.0	-1.3	-11.0	-22.6	-22.6	-17.5	-10.5	-5.4	-1.5	-0.8	-0.3	3.1
7	0.5	0.8	0.3	-9.0	-21.1	-22.6	-15.4	-7.4	-3.1	-1.3	0.0	0.3	2.3

that for Con 2, does not imply that further integration would have altered these conclusions, nor does a comparison of year 4 with the 3-year average.

4.6. Effect of Colder Sea Surface Temperatures

The radiative imbalance indicated in Table 3, and the net surface heating deficits over the North Atlantic for experiment 4 shown in Figure 14, indicate that had the model been allowed to run to equilibrium with reduced CO_2 , ocean temperatures would have cooled substantially (with a global cooling of approximately 2.5°C). In lieu of running the experiment for this length of time, we simply lowered the sea surface temperatures by using the values indicated for the LGM [CLIMAP Project Members, 1981]. This reduces the annual, global average ocean/sea ice surface temperature by 3.45°C (as we have also increased the sea ice accordingly) and lowers the global temperature by the required amount. Although there is no evidence that full ice age conditions existed in the North Atlantic during the time of ice growth, previous experiments [Rind, 1987a; Rind et al., 1986] have indicated that a colder ocean is more beneficial to ice maintenance, and the CLIMAP reconstruction represents at least an approximation to conditions that did exist during an ice age. The procedure for generating monthly average sea surface and sea ice conditions from the CLIMAP data set, and the values used, are given by Rind [1987a].

The resulting surface air temperature in experiment 6 was in approximate agreement with what would have been expected had experiment 4 been run to equilibrium. The surface air temperature change during summer, net heat at the surface, and mass balance are shown in Figure 15. Temperatures over the North Atlantic are considerably lower, while temperature reductions over land are greater primarily in the regions surrounding the ocean. For example, greater cooling occurs over western and northern Europe, over Greenland, and over Labrador and Baffin Island than in the previous experiments (compare with Figure 9). Net heating at the surface shows some reduction over North America in the vicinity of the Arctic circle, with much greater reductions over northwestern Europe, but it is still

positive in most of the regions of suspected ice sheet nucleation. The net moisture balance is still basically negative southward of 75°N , although there is some improvement over Baffin Island and northwestern Europe. From the mass and energy balance perspective, ice sheet maintenance would appear possible only over a small area of Baffin Island. Snow remains through July only over extreme northeastern Baffin Island, and eastern Scandinavia. On the latitudinal average, the ice still disappears in about 5 years (Table 4).

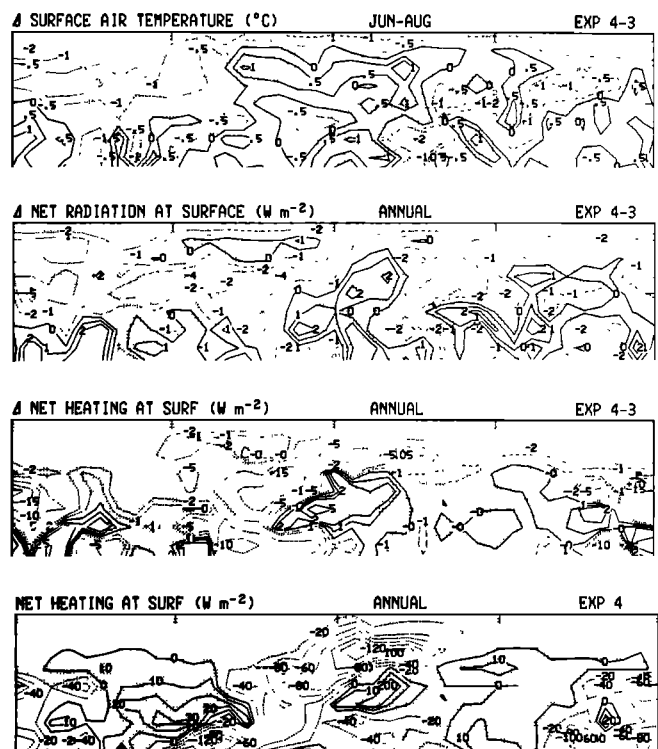


Fig. 14. Change in summer surface air temperature, and annual average net radiation at the surface, and net heating at the surface for experiment 4 (106 kyr B.P. insolation) minus experiment 3 (MIR). Also shown is the annual net heating at the surface for experiment 4.

Finally, as discussed by *Rind and Peteet* [1985], there is some evidence that the ice age climate was colder than is simulated by this model using the *CLIMAP Project Members* [1981] sea surface temperatures. When sea surface temperatures are reduced by 2°C below the CLIMAP values, better agreement is obtained. The greater reduction also brought the 18 kyr B.P. model into better radiative balance. The same holds true in these experiments: despite the reduction in sea surface temperatures, experiment 6 is still out of balance (Table 3) (i.e., would still cool by several degrees) because the increase in sea ice produces a larger albedo, so more solar radiation is reflected away. A further 2°C cooling, without large additions of sea ice, would be needed to achieve radiative balance.

Thus as a final attempt, we reran experiment 6 with a reduction in the CLIMAP 18 kyr B.P. ocean temperatures by 2°C, as experiment 7. The model was now in approximate radiation balance (Table 3). Melting rates for the latitude as a whole are reduced by about 30% (Table 4). Summer temperatures are reduced somewhat (Figure 16), especially in regions downstream of the open, colder waters. The net radiation and mass balances (Figure 16) are slightly more favorable for ice sheet maintenance over Baffin Island. For eastern North America, ice sheets would still melt in all but the very restricted regions noted above. The extensive sea ice in the western North Atlantic in the CLIMAP data set restricts the influence of colder ocean waters in that vicinity. This experiment shows that simply cooling the ocean waters somewhat more will not have a very large effect on ice sheet growth in eastern Canada.

5. DISCUSSION

The basic model experiment on the ability of Milankovitch variations by themselves to generate ice sheets in a GCM, experiment 2, shows that in the GISS GCM even exaggerated summer radiation deficits are not sufficient. If wide-

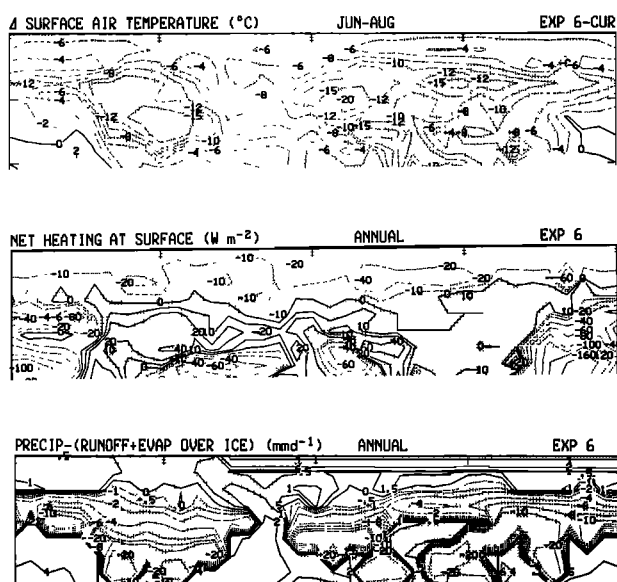


Fig. 15. (Top) Change in summer temperature, experiment 6 (CLIMAP ice age ocean) minus model current climate values for summer, (middle) annual net surface heating in experiment 6, and (bottom) annual net mass balance over land ice in experiment 6.

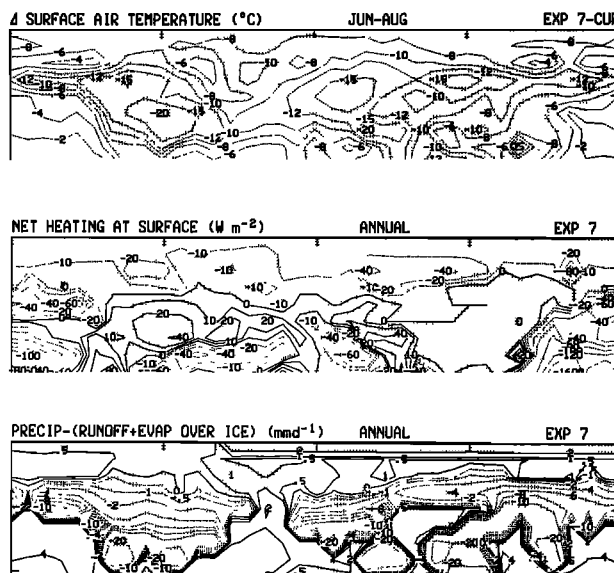


Fig. 16. As in Figure 15 except for experiment 7 (CLIMAP ice age ocean temperatures reduced by 2°C).

spread ice sheets at 10-m elevation are inserted, CO₂ reduced by 70 ppm, sea ice increased to full ice age conditions, and sea surface temperatures reduced to CLIMAP 18 kyr B.P. estimates or below, the model is just barely able to keep these ice sheets from melting in restricted regions. How likely are these results to represent the actual state of affairs?

While the reason(s) for reduced CO₂ levels during glacial regimes is not known, it appears that CO₂ reduction proceeded with ice growth, rather than preceding it [*Lorius et al.*, 1988]. The reduction of 70 ppm used in these experiments reduced the CO₂ value to about 240 ppm, a value that appears in the ice-core record at about 110 kyr B.P., lagging the isotope-deduced cooling (Figure 3; see also *Barnola et al.* [1987]). If CO₂ reductions did not occur prior to ice sheet growth, then experiments 2 and 3 are still the operative ones, at least from a global energy balance perspective, and there would be no obvious reason for the oceans to cool prior to ice sheet growth.

In order for the ice sheets to be maintained, even in restricted regions, full ice age ocean conditions had to be employed. *Ruddiman et al.* [1980] compared planktonic and benthic forams during stadial and interglacial time intervals, and concluded that North Atlantic sea surface temperature changes generally lagged behind ice growth, remaining warm for some 1000–5000 years after ice was accumulating on land. They hypothesized that this was the necessary condition for ice sheet growth, as the warm waters would provide the temperature contrast, and the moisture, necessary for storms to deposit snow. In these experiments, in agreement with full ice age simulations [*Rind*, 1987a], this scenario simply does not work in the GISS GCM; the annual average precipitation still decreases above the ice sheets (Figure 12), the warmer oceans lead to much greater melting, and the net mass balance change is negative. And while *Ruddiman and McIntyre* [1979] report a 3000–4000 year lag between apparent ice sheet growth, as determined from $\delta^{18}\text{O}$ variations, and sea surface temperatures in the North Atlantic, during stage 5, the sea surface temperatures do cool to only about one-half the full glacial depression by 106 kyr B.P.

Manabe and Broccoli [1985] have shown that the full glacial ice sheets with a simple ocean model could produce cooling which matched the CLIMAP sea surface temperature reductions in the extratropical Atlantic, to first order. Thus some observations and modeling studies imply that the ocean cooled after or at best in phase with ice sheet growth, not prior to their development.

The basic model scenarios (experiments 2 and 3) are thus the most likely ones. The inability of the GCM to produce the expected ice sheet initiation or maintenance raises several possibilities. The model may simply be inaccurate and respond with the wrong sensitivity to orbital forcing. This would obviously have implications for model projections of climate change. Or there may have been additional forcing mechanisms which were responsible for ice sheet initiation, not included in these experiments. Or possibly ice sheets did not start growing at this time, or they do not have as strong a connection with Milankovitch forcing as supposed. We discuss each of these possibilities separately.

5.1. Modeling Dependencies of the Results

How accurate is the GISS model for today's climate with respect to the current ice sheets? The model is currently in near energy balance over both polar ice sheets, with annual melting/growth rates of less than 10 cm/yr for Greenland/Antarctica. While we are not sure what the actual situation is for these ice sheets, the model values are consistent with present estimates [*U.S. Department of Energy*, 1985]. The current ice sheets are generally at higher latitude than the ice input in these ice initiation experiments, and perhaps more important, they are at a much greater elevation. The greater thickness results in less atmosphere above, and reduces the total concentration of greenhouse gases between the ice sheet surface and the top of the atmosphere. This allows long wave radiation to more easily escape, producing a more favorable energy balance. The height of the current ice sheets is one factor that allows them to be maintained.

How well does the model do in melting snow in summer in these regions? In Figure 17 we compare the model's snow cover with satellite-derived snow cover frequencies from 15 years of data [*Matson et al.*, 1986]. The data are impacted by cloud cover and other problems; nevertheless, the model appears to reduce snow cover too rapidly (in June) north of 60°, and to maintain too little snow cover over Baffin Island. There are at least two possible reasons for these discrepancies. The coarse resolution (8°) of the model grid box means that locations in the northern part of the grid are affected by warming which occurs to the south (see Figure 18 for grid box locations). As snow disappears uniformly in the grid box, this is equivalent to an infinitely fast diffusion of heat northward for 8° of latitude on entering summer. Furthermore, the model also has excess eddy energy in summer [*Hansen et al.*, 1983], which may lead to increased variability and snow removal. Both are factors which could bear on the questions discussed here.

The 4° × 5° version of the GISS model has both a finer resolution grid (Figure 18) and reduced eddy energy [*Rind*, 1988]. The comparison in Figure 17 shows that it produces more realistic snow cover north of 60°, although Baffin Island snow cover frequencies are still somewhat small in mid-summer. The temperature differences in summer between the two versions of the model are only several degrees

at most, and it is apparently a combination of this small reduction in temperature and the greater spatial differentiation available at higher resolution which accounts for the greater fine grid summer snow cover. At least part of the temperature difference may be associated with the slightly greater topography available with the finer resolution averaging; for example, in the 8° × 10° model, Baffin Island has an elevation of 180 m, while in the 4° × 5° version its elevation increases to 280 m. In reality, the Baffin Bay plateau has an elevation of about 576 m; *Birchfield et al.* [1982], using an energy balance climate model with an ice sheet model, have discussed the importance of topography in ice sheet generation. Apparently, the 4° × 5° model still does not have sufficient resolution to provide the proper topography and snow cover for Baffin Island, although it is obviously an improvement.

To determine the influence of the summer snow melting and the resolution in general, experiment 4 was redone with the finer resolution model. The results of this experiment initially mimic some of the characteristics which appear in the control runs, with the finer resolution version of experiment 4 having more snow cover at latitudes north of 60°; in June and July, the difference is most obvious over Baffin Island (as were snow depths in the control runs). The ice melting rates are still substantial, with the finer grid values being about 20% smaller than for the medium grid. However, the radiation imbalance at the top of the atmosphere is actually positive (by 2 W m⁻²), so this run would have warmed substantially had it been run to equilibrium. As discussed by *Rind* [1988], the fine grid atmosphere cools more when given ice age boundary conditions, due to reduced moist convection, so its cooler atmosphere radiates less energy to space, which accounts for the radiation imbalance being positive. Given that this resolution model already has substantial ice melting rates, with the additional warming that could be expected were it run to equilibrium (of some 2°C), it is clear that improving the resolution and the ability of the model to simulate snow cover during summer does not allow snow or ice to be maintained.

As indicated above, the increase in topography which results from averaging over smaller grids allows snow to persist in the Baffin Bay area. However, this region is anomalous in that respect. With the exception of a small area in Labrador (at approximately 54°N, 65°–70°W), there is no other region in the vicinity of Hudson Bay or eastern Canada that significantly increases in altitude as resolution decreases. Most areas are 100–300 m in altitude in both resolutions and in reality, a low elevation, which makes it difficult for snow or ice to persist with either resolution.

What about the model's depiction of sea ice, which will affect heat and moisture fluxes? In the specified sea surface temperature runs, sea ice is specified from climatology as well, but when the ocean temperatures are allowed to adjust, the model forms its own sea ice. As shown by *Hansen et al.* [1984], the model-generated sea ice for the current climate is, perhaps, 10–15% too small (although current sea ice locations are not precisely known). Given the relatively minor influence that the full ice age ocean conditions, including greatly expanded sea ice, had on the energy and mass balances, it is unlikely that the model tendency toward underestimating sea ice by this magnitude would have had much influence in the climate change experiments.

Hudson Bay is potentially an important exception to this

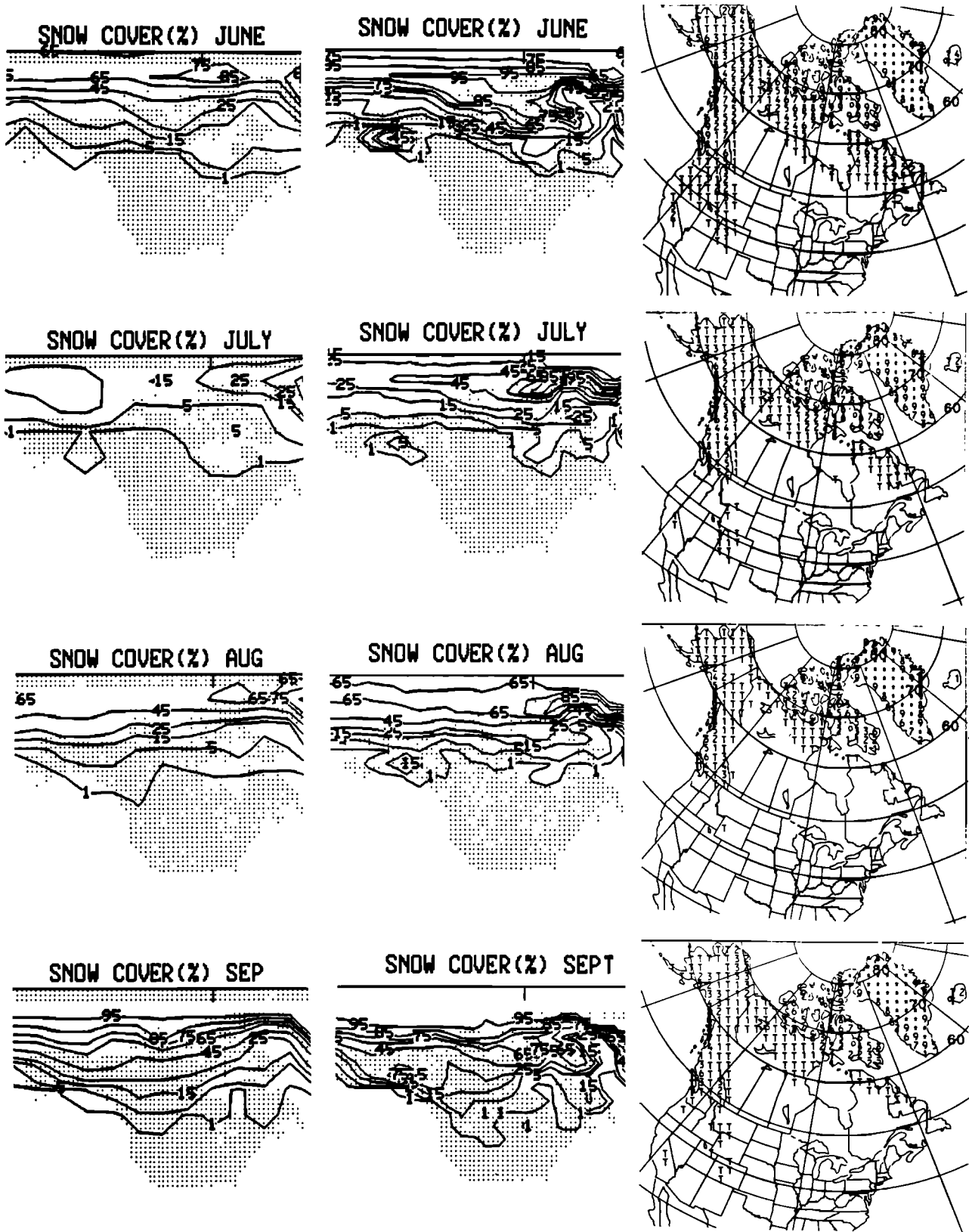
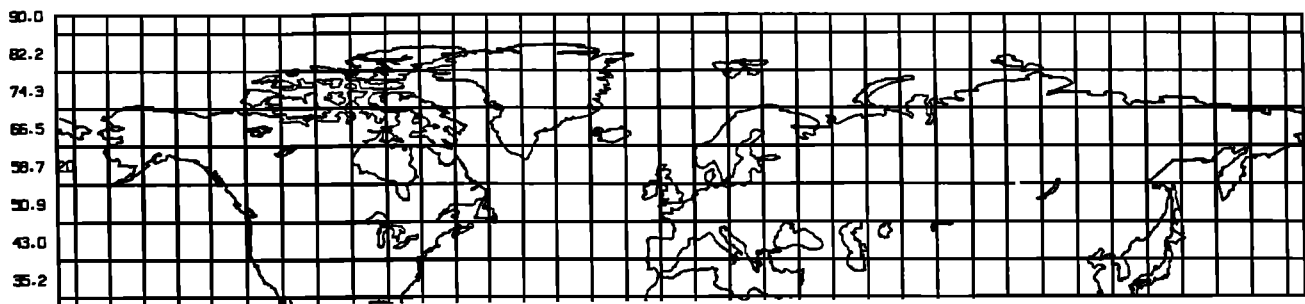


Fig. 17. Summer monthly snow cover frequency for the (left) 8° × 10° grid model, (middle) the 4° × 5° model, and (right) from satellite observations [Matson *et al.*, 1986]. For the observations, T indicates snow cover frequencies of 1-10%, 1 is 11-20%, etc.

PRIMARY GRID : MEDIUM RESOLUTION 7.83 X 10.00 DEGREES



PRIMARY GRID : FINE RESOLUTION 4.00 X 5.00 DEGREES

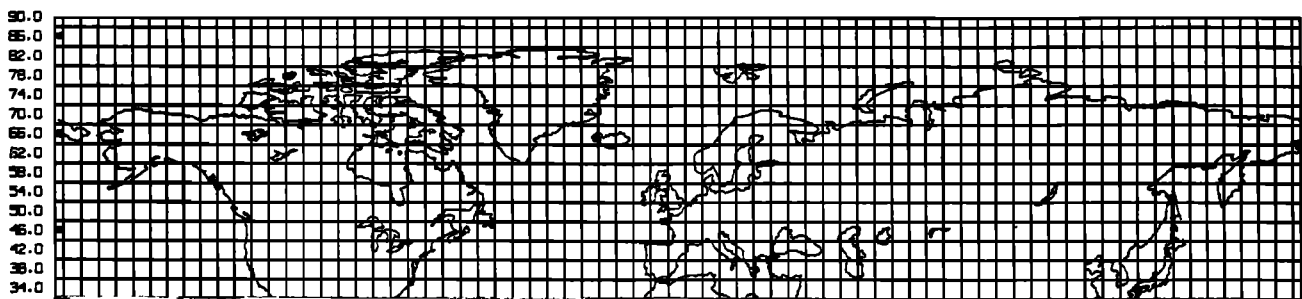


Fig. 18. Primary grid locations (for temperature, pressure, and precipitation) poleward of 30°N for (top) the 8° × 10° resolution model and (bottom) the 4° × 5° model.

conclusion, as it lies right in the middle of the area in question. The GCM includes “fractional grids,” with the percentage of water, land, and sea ice used separately for each grid box. In the 8° × 10° resolution model, Hudson Bay occupies portions of three grid boxes with the water plus sea ice fraction varying from 65–75% in each, as well as a smaller portion of a grid box to the south (Figure 18), while Hudson Strait represents 25% of a fifth grid box. The climatological sea ice field indicates that 1/3–2/3 of this water is ice covered during summer currently. When the model is allowed to generate its own sea ice (for the current climate), it produces summer values of 1/4–2/3 sea ice cover, again a slight underestimate. In climate change experiment 2, 15–85% of the water is ice covered in summer, indicating that the open water can provide a moderating effect; however, given the normal seasonal lag, the water temperatures are colder than nearby land temperatures and have reduced sensible heat fluxes. The fact that the Hudson Bay area is not completely ice covered in this experiment is due to the summer temperatures not being cold enough, the same reason that snow cover does not persist.

When considering the 10-m land ice experiments, a choice had to be made concerning the possibility of Hudson Bay being an open water body and thus providing a valuable source of moisture to maintain the ice, or, conversely, being ice covered to increase continentality. In the experiments in which sea surface temperatures were computed (experiments 3–5), Hudson Bay was not covered by the 10 m of land ice. The calculated conditions showed it developed 50–100% sea ice cover, and its surface fluxes did not differ from those

of surrounding grid boxes. For the runs with 10-m land ice and specified sea surface conditions (experiments 6 and 7), the opposite approach was taken, and the Hudson Bay surface was kept very cold (at -10°C). Surface fluxes were slightly reduced in its vicinity, as was the surface air temperature in summer. As ice would not be maintained over the Hudson Bay vicinity in any of the experiments, the choice did not dominate the results. Further uncertainties exist concerning the geographical makeup of this region prior to the last ice age.

One feedback which arises in the model is that as snow and ice cool the ground, the sensible heat loss to the atmosphere is reduced. This provides a negative feedback, as shown in Figure 11 for experiment 3. The sensible heat flux parameterization is based on a Richardson number criterion (section 2) derived from observations. As atmospheric stability increases, the eddy transfer coefficient decreases [Hansen *et al.*, 1983]. When snow or ice is present, the surface is kept cold, increasing stability, and reducing energy transfers. If the functional relationship between turbulence and the Richardson number is inaccurate, it could influence the sensible heat transfer response.

To test this possibility, the following modification was utilized in a rerun of experiment 4. When the Richardson number became negative, its value was automatically multiplied by a factor of 10. This has the effect of allowing significant sensible heat transport under slightly unstable conditions, in contrast to the usual formulation. Nevertheless, the effect does not produce noticeable differences, and the ice melting rates are not significantly altered. The results

from this experiment prove that the balance above ice sheets is not sensitive to this formulation. Apparently the presence of ice or snow makes the lower atmosphere in the model absolutely stable, in which case increasing the turbulent coefficient would transfer heat into the ground, melting ice faster. As the change made to the formulation was somewhat extreme, it is not obvious what realistic alterations of the surface physics could make the model more sensitive to radiation changes.

The current model produces too warm summer surface air temperatures in Antarctica [Hansen *et al.*, 1983]. A likely cause of this error is the albedo formulation for snow cover, in which snow albedo decreases as the snow ages (section 2, equations (6), (7)). The relationship was derived from observations over the western United States [U.S. Army Corps of Engineers, 1956] and seems to work well for most regions in the model. However, the same formulation produces surface albedos over Antarctica in summer as low as 60%, compared with observations of 80–90% [Carroll and Fitch, 1981]. In Antarctica, temperatures do not generally get above freezing even during the summer, so ice melting is not initiated. A strong component of the reduction of snow albedo with snow age may be the gradual melting of the snow surface, which may decrease the snow albedo by increasing the effective grain size [Wiscombe and Warren, 1980]. As the model surface albedo over Antarctica is too low, solar radiation is too effective in raising the surface air temperature.

To rectify this problem, and investigate its effect on ice melting in these experiments, a formulation was adopted in which snow only ages (and snow albedo decreases) when melting occurs [Jouzel *et al.*, 1987]. With this change, the control run produced accurate summer surface air temperatures over Antarctica, with little impact elsewhere. The same formulation was then used in a rerun of experiment 4. Once again there was little difference in result, presumably because the temperatures at the latitudes of interest were sufficiently high to initiate ice melting and snow aging.

Satellite observations of albedos over ice sheets and glaciers may be some 20% higher than those used in this model (C. Brest, personal communication, 1989), although separation of low clouds over ice sheets is extremely difficult. While most of the observations are for higher latitudes and altitudes, and thus uncertain analogs for the low lying ice sheets, as a somewhat extreme experiment, we increased the ice albedo to 90% in the visible and 70% in the near IR and did not allow snow to age, even if it was melting. Surface albedo increased by 25–30%, but the planetary albedo changed by only about 10% (due largely to the presence of atmospheric absorption in the visible), and ice melting rates were reduced by only 25%.

Cloud formation is handled crudely by current models. The spectrally integrated low cloud albedo is close to 50% in the model. If this were to increase by 20%, it would help to alleviate the ice melting problem. Satellite observations imply that the model's values are too high for the current climate (B. Rossow, personal communication, 1989).

Sommerville and Remer [1984] suggested that cloud cover optical thickness might vary with the atmospheric saturation specific humidity and thus the temperature. In colder climates, with less atmospheric moisture content they would then thin (optically), which would reduce their albedo. This effect is by no means certain to occur in the real world, but if it did, it would work against ice sheet growth.

Nevertheless, the possibility exists that the model's inability to maintain the ice sheets could be associated with the albedo of the ice/low cloud system. With higher snow/ice albedos, or thicker clouds, the total reflectivity could conceivably be high enough to protect the ice sheets. J. Pollack (personal communication, 1989) suggested that snow may have had fewer impurities and thus higher albedos at these times. More research is needed in this area, although the lack of current-day analogs will complicate any interpretations.

An additional model deficiency relates to its treatment of the oceans. These experiments assumed that ocean transports would not change. If ocean circulation changed drastically, perhaps due to reduction in North Atlantic Deep Water production, then significant ocean cooling might arise prior to ice sheet development. Broecker *et al.* [1985] suggested this as a possible mechanism for rapid climate change. Duplessy *et al.* [1988] used δC_{13} values from marine organisms to conclude that a large cessation of North Atlantic Deep Water formation did not occur until about 75 kyr B.P., long after the ice buildup presumably occurred.

Once ocean ice age conditions are established, increased sea ice could help limit deep-water production, by capping ocean heat ventilation, and changing the precipitation/evaporation balance. Again this mechanism would require the ocean to cool prior to ice sheet development for it to play a role in these experiments, and the annual net radiation balance does not vary sufficiently with the changed orbital parameters to suggest such a cooling from radiative effects alone. As noted above, observations of isotopic variations in marine organisms seem to indicate that ocean cooling occurred in conjunction with ice sheet growth (perhaps due to a change to more northerly winds associated with high-pressure development over the ice sheets), rather than preceding it. In particular, at this time period, faunal evidence of sea surface temperature cooling lags the isotope evidence of ice sheet growth by some 5000 years [Ruddiman and McIntyre, 1979].

The experiments performed here did not utilize an ice dynamics model. G. E. Birchfield (personal communication, 1988) has found that spatial finite differencing of the order of approximately 20 km was necessary for his ice sheet model to resolve ice growth in certain situations. Without reference to models on these scales, it is possible the GCM could underestimate ice sheet growth, although the large-scale conditions for sustaining the input 10-m ice sheets are so unfavorable that it is questionable whether ice could have survived in more sophisticated models. Further investigations in this area would seem worthwhile.

Even if there is no obvious specific reason why the model should have failed to grow ice sheets, the possibility still remains that the model as a whole is too insensitive to climate perturbations, or at least its high-latitude response. This would have to involve the magnitude of the feedbacks which accompany the climate forcing (e.g., water vapor, cloud cover), not only over the ice sheets but perhaps everywhere. As the reduced CO₂ experiment was not actually run to equilibrium, there is the possibility that had it been, it would have produced results quite different from the full ice age conditions which were utilized instead, in experiments 6 and 7. Given the model's tendency to produce less high-latitude amplification of temperature change than is implied by the CLIMAP data set [Rind, 1988], it is likely the

model would have ended up with warmer ocean temperatures at high latitudes than used in those experiments; as noted above, this effect would have melted ice even faster. If the global response is really inaccurate, it would have important implications for our use of such models to evaluate potential future climate changes resulting from increased CO₂. If its high-latitude amplification of climate change is underestimated, it would have important implications for projected atmospheric dynamic and regional climate changes [Rind, 1987b].

5.2. Additional Potential Forcing Functions

What physical forcing mechanisms have been left out of these experiments which could influence the results? Ledley [1984] and Neeman *et al.* [1988], using energy balance models, suggested that additional cooling mechanisms were necessary to account for ice sheet growth. Increased atmospheric turbidity due to drier and colder conditions could affect solar radiation. Hansen *et al.* [1988] compared the magnitude of different radiative forcings and found that an increase in sulfuric acid particles in the lower stratosphere could have an appreciable effect. The aerosols associated with a cold dry climate would be more like desert aerosols, which would have a much smaller radiative impact. Furthermore, the climate would have to cool and dry first, and the solar radiation variations do not generate cooler and drier conditions in all seasons (e.g., Figure 5). Observations of dust in the Vostok ice core indicate it did not apparently increase until about 60 kyr B.P.; in particular, at 110 kyr B.P. there was no apparent increase in tropospheric aerosol loading [de Angelis *et al.*, 1987].

Were volcanic eruptions to increase substantially in conjunction with orbital variations, an increased cooling effect could result. Bray [1977] attempted to find such a correlation using ocean ash data, and discussed records which implied that volcanism increased during the temperature maxima preceding the rapid cooling. However, the margins of error associated with dating uncertainties are such that no firm conclusion can really be drawn about any relationship.

The only other obvious potential forcing function is the solar constant itself. Were solar intensity to vary with orbital time scales, it could obviously initiate ice ages given a large enough magnitude variation. Current models show that a 2% solar increase produces the same climate response as doubled atmospheric CO₂ [Hansen *et al.*, 1984]. From these experiments, we estimate that global temperatures would need to decrease by at least 8°C (the difference between experiment 7 and today in July), which would imply, with the GISS model sensitivity, a reduction in solar constant by some 4%, in addition to the orbital-induced temperature changes (Figure 5). There is no evidence that such a reduction did take place, and it would have to occur in apparent conjunction with orbital variations. On the longer time scale (i.e., 150–300 m.y.), the passing of the solar system through interstellar clouds has been suggested as a possible cause for ice ages [e.g., Yabushita and Allen, 1985].

5.3. The Question of Early Wisconsinan Ice

Where was ice during the early Wisconsinan (120–100 kyr B.P.), and how much was there? Perhaps the model's

inability to grow ice except possibly over Baffin Island is indicative of what the actual conditions were. A recent conference, "The Last Interglaciation/Glaciation Transition" (at the Geological Society of America (GSA) annual meeting, October 30, 1988, in Denver, Colorado) tended to deemphasize the growth of ice in the early Wisconsinan. Nevertheless, the marine isotope variations (e.g., Figure 3) show changes during the 120–100 kyr B.P. time period, about 1/2 of that from the interglacial to the full glacial, and temperature indicators from both Antarctica and Greenland show rapid cooling at this time. If the proportion of isotope change that is contributed by ice volume increase (as opposed to ocean cooling) is the same in the early and late Wisconsinan, and the CLIMAP estimate of 125-m reduction in sea level at the Last Glacial Maximum is correct, then the isotope record implies a sea level drop of some 60 m at the time period of these experiments. This amount is too large to be sequestered in a tiny area such as Baffin Island; Andrews and Mahaffy [1976] estimated that only 3 m of sea level drop could be associated with the growth of ice in this area during the early Wisconsinan.

Various presentations at the GSA conference addressed the question of early Wisconsinan ice location. Miller and Andrews [1988] suggested it was possibly confined to extreme northeastern Canada, Baffin Island in particular. Vincent [1988] suggested that ice started west of Hudson Bay and flowed toward the Beaufort Sea. Thorleifson *et al.* [1988] placed ice on the lowlands south of Hudson Bay, again flowing northwestward. All of these estimates are hard to place temporally, due to uncertainties in dating. They indicate the question of early Wisconsinan ice extent and location is still an open one.

Does the isotope curve really indicate such a large magnitude of ice sheet growth at that time? Coral records for sea level depression during isotope stages 5c (~100 kyr B.P.) and 5a (~80 kyr B.P.) indicate a drop of only 9–19 m [Chappell and Shackleton, 1986], while linear translation of the marine isotope curve based on glacial/interglacial changes would suggest sea level depression of twice these values. Either the isotope composition of ice changed with time or ocean temperature changes had relatively greater effect on the marine isotope records during stage 5 than during the glacial maximum. Planktonic records of $\delta^{18}\text{O}$ depression show a smaller peak at 5e (the previous interglacial) than do the benthic values in Figure 3, implying that deep-ocean temperature changes may have been more important than sea surface temperature changes, contrary to expectation.

Chappell and Shackleton [1986] tried to deconvolve the sea level depression from other factors in the isotope record, by comparison with coral terrace data in the New Guinea/Australian region. Their reconstructed sea level curve still shows significant sea level depression around 110 kyr B.P. of close to 50 m, assuming that the full glacial sea level reduction was 130 m. Even the full ice age value is uncertain, with ranges from 80 to 150 m extant in the literature, and were the full glacial maximum value to be overestimated, so would the drop during stage 5. Nevertheless, with our current understanding, it appears as if the model should have been able to sequester a substantial amount of ice in the early Wisconsinan. Note also that without reduced CO₂, the insolation change did not even initiate any large global cooling (Table 3).

The possible importance of marine ice transgressions in initiating the growth of ice sheets has been raised [Denton and Hughes, 1981; Hughes, 1987]. In this scenario, the permanent Arctic Sea ice extends southward into interisland channels and marine embayments on the polar continental shelves, forming high albedo surfaces on which snow can accumulate to eventually produce ice shelves. One can hypothesize that such a process, in addition to localized mountain glacier generation, might have been responsible for the 50-m sea level reduction. While the GCM does not contain a sophisticated sea ice model, the results from experiment 3 do not indicate full sea ice coverage during summer in either the interisland channels or Hudson Bay, with values generally ranging between 30% and 80%.

5.4. Milankovitch Variations and Ice Sheet Growth

The correlation of isotope indications of ice sheet growth and Milankovitch variation decreases in summer solar radiation at high northern latitudes (Figures 1 and 3) produces a first-order correspondence between ice growth and orbital periodicity patterns (although the timing of the isotope changes is to some extent tuned to the orbital variations). However, the amplitudes of the orbital variations do not match the magnitude of continental ice sheets. For example, the most extreme reduction in summer radiation occurs around 110 kyr B.P., the next most extreme around 90 kyr B.P., and the least extreme around 20 kyr B.P. This is in direct opposition to the total ice loading suggested by the isotope curve.

The only feature of the insolation record that conceptually supports maximum ice sheet growth near 20 kyr B.P. is the lack of a large insolation maximum for the previous 60,000 years (i.e., until 80 kyr B.P.). Nevertheless, the mid-summer values from 60 to 20 kyr B.P. are all similar to or greater than today's insolation. If the insolation at 10 kyr B.P. (Figure 1) was sufficient to melt ice sheets rapidly, it is not obvious that the values at 60 kyr B.P. would not be also, and if ice really did melt at that time, there are no large insolation minima to provide stimulus for the Last Glacial Maximum. At the very least, this suggests the importance of the maximum CO₂ reduction between 50 and 20 kyr B.P. (Figure 3) in generating the full-scale global cooling. A scenario in which small initial cooling (and subsequent amplifications) is associated with summer solar radiation deficits, but the main cooling is associated with CO₂ reductions, is then consistent with this picture, though not necessarily with the isotope evidence (Figure 3) which implies relatively large and rapid cooling prior to any CO₂ reduction around 110 kyr B.P. Nor, of course, does it explain why the CO₂ decrease occurred in possible conjunction with the cooling.

These comments serve to highlight the model's inability to grow ice with stage 5 radiation values. If the model would not initiate or sustain low-altitude ice at around 110 kyr B.P., it is unlikely it would do so at any time between then and 18 kyr B.P., as no other radiation condition is obviously more favorable. Certainly the values between 60 and 20 kyr B.P. would not work. If ice sheets had attained a greater thickness in this interval, the model may have supported them, for, as noted earlier, the greater thickness reduces the greenhouse gas concentration in the atmosphere above. But they still presumably would have had to grow from thinner

ice sheets, which the model would not have sustained. Even increased cooling, consistent with 70 ppm CO₂ reduction, used in experiments 6 and 7 was not sufficient to sustain ice over wide areas.

How high would the ice sheets we inserted into the model have had to be before they would have been maintained for the conditions of experiment 3? We can provide a very crude estimate by noting that with the 18 kyr B.P. radiation and sea surface temperature conditions, the 2.5-km ice sheets melted some 500 mm/yr faster than did the 10-m ice sheets [Rind, 1987a]. If the same relationships apply to the altered radiation condition, and if the variation of ice sheet melting with altitude is linear, then to reduce the melting rates in Table 4 to zero would require ice sheets of at least several kilometers' thickness, even for experiment 7. While these assumptions are not likely to be completely correct, the results imply that thick ice would be required before it could be sustained in the model's ablative environment, much thicker than piedmont glaciers would likely be when exiting highland regions, or than the proposed marine ice sheet domes (of 20 m [Hughes, 1987]).

One problem with the orbital induced radiation changes is that summer deficits are often accompanied by springtime surpluses, which are effective in melting ice (Table 4). Comparison of the marine isotope curve and the insolation variations indicates maximum ice growth seemed to coincide with reduced northern hemisphere insolation during the middle and late summer and fall periods. It was just this effect that the modified insolation field used here was intended to amplify; but again, in amplifying the late summer decrease, it also exaggerated the springtime increase. Nevertheless, even the reduced summer values were sufficient to promote substantial ice melting during August, especially without ice age sea surface temperatures (Table 4).

It is often mentioned that the apparent in-phase growth of ice in the northern and southern hemispheres is in direct contrast with the solar radiation record of opposing tendencies of summer radiation in the two hemispheres. In fact, this is true only of the 23,000-year cycle; obliquity variations with 40,000-year periodicity are in phase at high latitudes. The solar insolation at 116, 64, and 22 kyr B.P. has summertime decreases at high latitudes of both hemispheres. Growth of ice on Antarctica could have been responsible for some of the sea level reduction which may have occurred in the early Wisconsinan. The model simulations do support the growth of ice at the highest latitudes in Antarctica, although there are slight reductions for the southern hemisphere as a whole. It is not at all clear that ice sheets did thicken in Antarctica, even during the full glacial maximum.

6. CONCLUDING REMARKS

One of the prime uses of models is to investigate hypotheses of cause and effect. When the models fail to produce the expected response to the input forcing function, either the model is wrong, the response is being misinterpreted, or the forcing function is not properly specified. The results of the experiments discussed here leave open all three possibilities.

We need to determine whether ice really started growing in the early Wisconsinan. Our inability to date glacial moraines back to 120 kyr B.P. prevents us from using the land evidence in an unambiguous manner; furthermore, subsequent glacial movement has eliminated much of the useful

evidence. Our inability to separate ice volume changes from ocean temperature changes in the oxygen isotope record introduces serious uncertainties into reconstructions of past sea level change. However, while we cannot say just how much ice really was present in stage 5, there is little doubt that major ice sheet growth did occur by 20 kyr B.P. It is unlikely that the GISS GCM could have produced that effect at anytime during the last 120,000 years with Milankovitch variations alone, and low-elevation ice would probably not have been sustainable south of 60°N even with reduced CO₂. If the model results are correct, they would emphasize the difficulty which ice sheets would have encountered when venturing out of mountain regions, which might be the cause for their apparently slow growth to full ice age conditions.

The relationship of Milankovitch orbital variations to ice ages is apparent in the geophysical record, through a general correlation of reduced northern hemisphere summer insolation with ice sheet growth and temperature cooling (as deduced from isotopic records). In addition, there is a coincidence of spectral frequency responses between orbital variations and paleoclimate indicators, although the large eccentricity forcing appears out of place. However, a closer analysis of ice sheet growth and maximization with the orbital record indicates the match is less convincing. The ice sheets did not maximize in what we currently understand to be the most favorable radiation conditions. This raises the possibility that other factors are necessary, and perhaps of even paramount importance, a result which is supported by the model's inability to grow ice sheets with even exaggerated orbital forcing. However, reduced CO₂ is an obvious candidate in this regard, but even temperature reductions consistent with 240 ppm CO₂ did not allow the model to sustain much low-altitude ice.

Finally, the possibility exists that the model is not nearly as sensitive to orbital variations as it should be. Such a result could have serious implications for studies of future climate, although since the nature of the insensitivity (if it exists) is unknown, its effect is uncertain. The model may simply not handle the ice/snow/low cloud albedo properly, either today or for paleoclimate times. In this case, model assessments of the change of ice balance for Greenland or Antarctica due to future greenhouse warming could be too small, or the snow albedo feedback miscalculated. The finer grid model represents summer snow cover more accurately at high latitudes but still produces substantial ice melting, and it is doubtful whether increasing the resolution further would change the conclusions. Alternatively, the model may just be too insensitive to any perturbation, either globally or in terms of its high-latitude amplification of temperature change; this would imply that estimates of the magnitude of climate change associated with doubled CO₂ would be too small, or the dynamical and regional distribution of climate change effects inaccurate. All the GCMs are currently producing similar responses to doubled CO₂ and to orbital parameter changes (e.g., 11 kyr B.P.), which suggests that other models are likely to have similar problems reproducing ice sheet initiation if they can remove snow/ice realistically today. It is obviously of great interest to resolve the apparent discrepancies suggested by these experiments.

Acknowledgments. We thank Gary Russell for help in producing the orbital variations of solar insolation, and Bill Ruddiman, Peter

Clark, Steve Porter, Dan Mann, Dick Stothers, and Jim Pollack for useful discussions. John Kutzbach and Edward Birchfield provided helpful comments in reviewing the manuscript. Climate modeling at GISS is supported by the NASA Climate Program Office.

REFERENCES

- Andrews, J.T., The Late Wisconsin glaciation and deglaciation of the Laurentide ice sheet, in *The Geology of North America*, vol. k-3, *North America and Adjacent Oceans During the Last Deglaciation*, edited by W. F. Ruddiman and H. E. Wright, Jr., pp. 13–37, Geological Society of America, Boulder, Colo., 1987.
- Andrews, J. T., and M. A. Mahaffy, Growth rates of the Laurentide Ice Sheet and sea level lowering (with emphasis on the 115,000 BP sea level low), *Quat. Res.*, **6**, 167–183, 1976.
- Barnola, J.-M., D. Raynaud, Y. S. Korotkevich, and C. Lorius, Vostok ice core provides 160,000-yr record of atmospheric CO₂, *Nature*, **329**, 408–414, 1987.
- Barry, R. G., J. T. Andrews, and M. A. Mahaffy, Continental ice sheets: Conditions for growth, *Science*, **190**, 979–981, 1975.
- Berger, A. L., Long-term variations of daily insolation and Quaternary climatic changes, *J. Atmos. Sci.*, **35**, 2362–2367, 1978.
- Birchfield, G. E., and J. Weertman, A model study of the role of variable ice albedo in the climate response of the Earth to orbital variations, *Icarus*, **50**, 462–472, 1982.
- Birchfield, G. E., J. Weertman, and A. T. Lunde, A model study of the role of high-latitude topography in the climatic response to orbital insolation anomalies, *J. Atmos. Sci.*, **39**, 71–87, 1982.
- Bray, J., Pleistocene volcanism and glacial initiation, *Science*, **197**, 251–254, 1977.
- Broecker, W. S., D. M. Peteet, and D. Rind, Does the ocean-atmosphere system have more than one stable mode of operation?, *Nature*, **315**, 21–26, 1985.
- Carroll, J. J., and B. W. Fitch, Effects of solar elevation and cloudiness on snow albedo at the South Pole, *J. Geophys. Res.*, **86**, 5271–5276, 1981.
- Chappell, J., and N. J. Shackleton, Oxygen isotopes and sea level, *Nature*, **324**, 137–140, 1986.
- CLIMAP (Climate: Long-Range Investigation, Mapping, and Prediction) Project Members, Seasonal reconstruction of the earth's surface at the last glacial maximum, *Map Chart Ser.*, **MC-36**, Geol. Soc. of Am., Boulder, Colo., 1981.
- de Angelis, M., N. I. Barkov, and V. N. Petrov, Aerosol concentration over the last climatic cycle (160 kyr) from an Antarctic ice core, *Nature*, **325**, 318–321, 1987.
- Denton, G. H., and T. J. Hughes, The Arctic ice sheet: An outrageous hypothesis, in *The Last Great Ice Sheets*, edited by G. H. Denton and T. J. Hughes, pp. 437–467, John Wiley, New York, 1981.
- Duplessy, J. C., N. J. Shackleton, R. G. Fairbanks, L. Labeyrie, D. Oppo, and N. Kallel, Deepwater source variations during the last climatic cycle and their impact on the global deepwater circulation, *Paleoceanography*, **3**, 343–360, 1988.
- Hansen, J., G. Russell, D. Rind, P. Stone, A. Lacis, S. Lebedeff, R. Reudy, and L. Travis, Efficient three-dimensional global models for climate studies. Models I and II, *Mon. Weather Rev.*, **111**, 609–662, 1983.
- Hansen, J., A. Lacis, D. Rind, G. Russell, P. Stone, I. Fung, R. Reudy, and J. Lerner, Climate sensitivity: Analysis of feedback mechanisms, in *Climate Processes and Climate Sensitivity*, edited by J. E. Hansen and T. Takahashi, pp. 130–163, AGU, Washington, D. C., 1984.
- Hansen, J., I. Fung, A. Lacis, D. Rind, S. Lebedeff, R. Reudy, and G. Russell, Global climate changes as forecast by Goddard Institute for Space Studies three-dimensional model, *J. Geophys. Res.*, **93**, 9341–9364, 1988.
- Hays, J. D., J. Imbrie, and N. J. Shackleton, Variations in Earth's orbit: Pacemaker of the ice ages, *Science*, **194**, 1121–1132, 1976.
- Hughes, T. J., The marine ice transgression hypothesis, *Geogr. Ann.*, **69A**, 237–250, 1987.
- Ives, J. D., J. T. Andrews, and R. G. Barry, Growth and decay of the Laurentide Ice Sheet and comparisons with Fenno-Scandinavia, *Naturwissenschaften*, **62**, 118–125, 1975.
- Jouzel, J., G. Russell, R. Suozzo, R. Koster, J. White, and W. Broecker, Simulations of the HDO and H₂¹⁸O atmospheric cycles using the NASA GISS general circulation model: The

- seasonal cycle for present-day conditions, *J. Geophys. Res.*, **92**, 14,739–14,760, 1987.
- Kukla, G., End of the last interglacial: A predictive model of the future?, in *Paleoecology of Africa and the Surrounding Islands*, edited by E. M. Van Zinderen Bakker, Sr. and J. A. Coetzee, pp. 395–408, A. A. Balkema, Rotterdam, 1980.
- Kukla, G., A. Berger, R. Lotti, and J. Brown, Orbital signature of interglacials, *Nature*, **290**, 295–300, 1981.
- Kutzbach, J., and R. G. Gallimore, Sensitivity of a coupled atmosphere/mixed layer ocean model to changes in orbital forcing at 9000 years B.P., *J. Geophys. Res.*, **93**, 803–821, 1988.
- Ledley, T. S., Sensitivities of cryospheric models to insolation and temperature variations using a surface energy balance, in *Milankovitch and Climate*, part 2, edited by A. Berger, J. Imbrie, J. Hays, G. Kukla, and B. Saltzman, pp. 581–598, D. Reidel, Hingham, Mass., 1984.
- Lorius, C., N. I. Barkov, J. Jouzel, Y. S. Korotkevich, V. M. Kotlyakov, and D. Raynaud, Antarctic ice core: CO₂ and climatic change over the last climatic cycle, *Eos Trans. AGU*, **69**, 681–684, 1988.
- Manabe, S., and A. J. Broccoli, The influence of continental ice sheets on the climate of an ice age, *J. Geophys. Res.*, **90**, 2167–2190, 1985.
- Matson, M., C. F. Ropelewski, and M. S. Varnadore, *An Atlas of Satellite-Derived Northern Hemispheric Snow Cover Frequency*, 75 pp., U.S. Department of Commerce, Washington, D. C., 1986. (Available from NOAA/NESDIS, E/RA22 5200 Auth Road, Washington, D. C. 20233.)
- Mesolella, K. J., R. K. Matthews, W. S. Broecker, and D. L. Thurber, The astronomical theory of climate change, *J. Geol.*, **77**, 250–274, 1969.
- Miller, G. H., and J. T. Andrews, Timing and characteristics of early Wisconsin ice sheet growth in NE Canada, *Geol. Soc. Am. Abstr. Programs*, **20**, A3, 1988.
- Neeman, B. U., G. Oehring, and J. H. Joseph, The Milankovitch theory and climate sensitivity, 2, Interaction between the northern hemisphere ice sheets and the climate system, *J. Geophys. Res.*, **93**, 11,175–11,191, 1988.
- Oerlemans, J., Model experiments on the 100,000 yr. glacial cycle, *Nature*, **287**, 430–432, 1980.
- Pollard, D., A coupled climate-ice sheet model applied to the Quaternary ice ages, *J. Geophys. Res.*, **88**, 7705–7718, 1983.
- Prest, V. K., The Late Wisconsin glacier complex, Quaternary stratigraphy of Canada; A Canadian contribution to IGCP Project 24, *Geol. Surv. Can. Pap.*, **84-10**, 21–38, 1984.
- Rind, D., Components of the ice age circulation, *J. Geophys. Res.*, **92**, 4241–4281, 1987a.
- Rind, D., The doubled CO₂ climate: Impact of the sea surface temperature gradient, *J. Atmos. Sci.*, **44**, 3235–3268, 1987b.
- Rind, D., Dependence of warm and cold climates on climate model resolution, *J. Clim.*, **1**, 965–997, 1988.
- Rind, D., and D. Peteet, Terrestrial conditions at the last glacial maximum and CLIMAP sea-surface temperature estimates: Are they consistent?, *Quat. Res.*, **24**, 1–22, 1985.
- Rind, D., D. Peteet, W. Broecker, A. McIntyre, and W. Ruddiman, The impact of cold North Atlantic sea surface temperatures on climate: Implications for the Younger Dryas cooling (11–10k), *Clim. Dyn.*, **1**, 3–33, 1986.
- Royer, J. F., M. Deque, and P. Pestiaux, A sensitivity experiment to astronomical forcing with a spectral GCM: Simulation of the annual cycle at 125,000 BP and 115,000 BP, in *Milankovitch and Climate*, part 2, edited by A. L. Berger et al., pp. 733–763, D. Reidel, Hingham, Mass., 1984.
- Ruddiman, W. F., and A. McIntyre, Warmth of the subpolar North Atlantic Ocean during Northern Hemisphere ice-sheet growth, *Science*, **204**, 173–175, 1979.
- Ruddiman, W. F., A. McIntyre, B. Niebler-Hunt, and J. T. Durazzi, Oceanic evidence for the mechanism of rapid Northern Hemisphere glaciation, *Quat. Res.*, **13**, 33–64, 1980.
- Schneider, S. H., and S. L. Thompson, Ice ages and orbital variations: Some simple theory and modeling, *Q. Res.*, **12**, 188–203, 1979.
- Sommerville, R. C., and L. A. Remer, Cloud optical thickness feedbacks in the CO₂ climate problem, *J. Geophys. Res.*, **89**, 9668–9672, 1984.
- Suarez, M. J., and I. M. Held, The sensitivity of an energy balance climate model to variations in the orbital parameters, *J. Geophys. Res.*, **84**, 4825–4836, 1979.
- Thorleifson, L. H., W. W. Shilts, P. H. Wyatt, and E. Neilsen, Early Wisconsinan glaciation of the Hudson Bay lowland, *Geol. Soc. Am. Abstr. Programs*, **20**, A4, 1988.
- U.S. Army Corps of Engineers, *Snow Hydrology, Report of Snow Investigations*, 437 pp. North Pacific Division, Portland, Oreg., 1956.
- U.S. Department of Energy, Glaciers, ice sheets, and sea level: Effect of a CO₂-induced change, *Rep. DOE/ER/60235-1*, 348 pp., Washington, D. C., 1985.
- Vincent, J.-S., The Sangamonian and early Wisconsinan record in the western Canadian arctic (abstract), *Geol. Soc. Am. Abstr. Programs*, **20**, A4, 1988.
- Williams, L. D., An energy balance model of potential glacierization of northern Canada, *Arct. Alp. Res.*, **11**, 443–456, 1979.
- Wiscombe, J. W., and S. G. Warren, A model for the spectral albedo of snow, I, Pure snow, *J. Atmos. Sci.*, **37**, 2712–2733, 1980.
- Yabushita, S., and A. J. Allen, On the effect of interstellar matter on terrestrial climate, *Observatory*, **105**, 199–200, 1985.

G. Kukla, Lamont-Doherty Geological Observatory of Columbia University, Palisades, NY 10964.

D. Peteet and D. Rind, Goddard Space Flight Center, Institute for Space Studies, 2880 Broadway, New York, NY 10025.

(Received October 20, 1988;
revised February 8, 1989;
accepted February 22, 1989.)